R. Zentel and E.-K. Fleischmann

DOI: 10.1002/anie.201300371

Liquid Crystals

Liquid-Crystalline Ordering as a Concept in Materials Science: From Semiconductors to Stimuli-Responsive Devices

*Eva-Kristina Fleischmann and Rudolf Zentel**

Keywords:
liquid crystals · materials chemistry · self-assembly · semiconductors

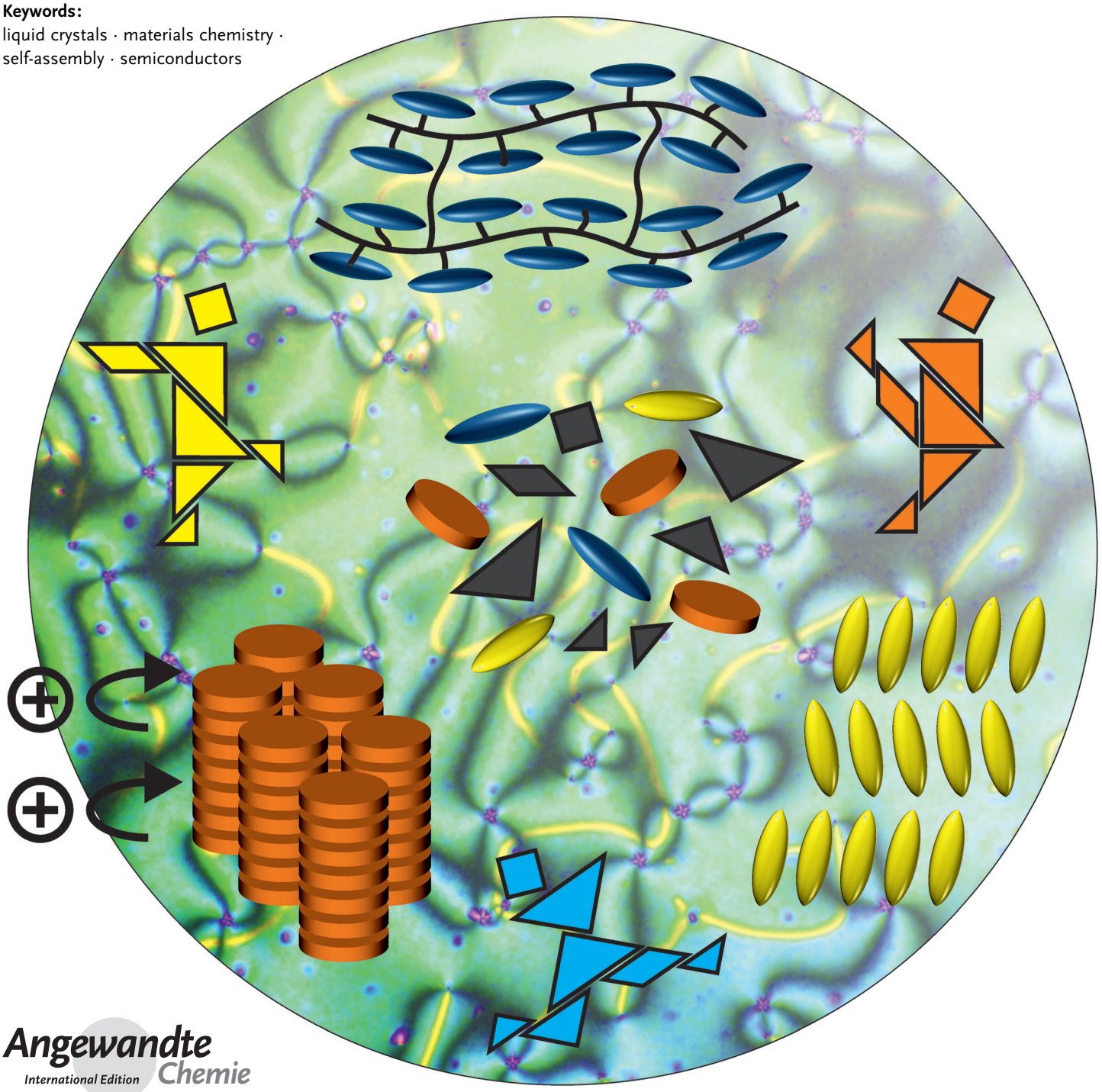

While the unique optical properties of liquid crystals (LCs) are already well exploited for flat-panel displays, their intrinsic ability to self-organize into ordered mesophases, which are intermediate states between crystal and liquid, gives rise to a broad variety of additional applications. The high degree of molecular order, the possibility for large scale orientation, and the structural motif of the aromatic subunits recommend liquid-crystalline materials as organic semiconductors, which are solvent-processable and can easily be deposited on a substrate. The anisotropy of liquid crystals can further cause a stimuli-responsive macroscopic shape change of cross-linked polymer networks, which act as reversibly contracting artificial muscles. After illustrating the concept of liquid-crystalline order in this Review, emphasis will be placed on synthetic strategies for novel classes of LC materials, and the design and fabrication of active devices.

From the Contents

1. Introduction

Since their first observation by botanist Friedrich Reinitzer in the late 19th century, liquid crystals have attracted the attention of chemists and physicists alike.[1–3] With their ability to self-organize into so-called mesophases, which combine order and mobility, they belong to the topical field of soft matter.[4] These mesophases are an intermediate state between the classical crystalline and isotropic liquid phases, and their macroscopic behavior is defined by the molecular properties of their constituents, the mesogens. The premise for the formation of a liquid-crystalline phase, which combines long-range order with the mobility of fluids, is the shape anisotropy of these mesogens. A distinction is made between calamitic (rod-like), discotic[5] (disc-like), sandic[6] (board-like), and banana-shaped mesogens[7] (Figure 1 A) and the corresponding phases. While a rigid core (which often consist of aromatic rings) induces structural order, flexible parts (for example alkyl chains) provide for the necessary mobility within the liquid-crystalline phase. Typical molecular building blocks and typical phase sequences are presented in Figure 1. In this context, it should be noted that not only organic compounds but also anisotropic inorganic nanoparticles form liquid-crystalline phases.[8,9] The necessary mobility for the stiff particles can be provided by a polymer coating resulting in organic–inorganic hybrid materials. Such materials with potential applications in the field of opto-electronics will be discussed in Section 2.4.

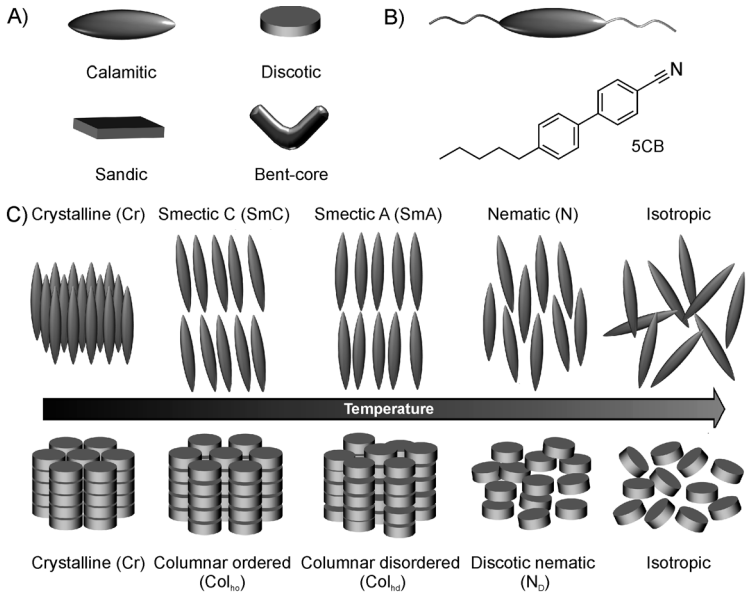

Figure 1. A) Shape-anisotropic cores of liquid-crystalline molecules. b) Top: Representation of a common class of liquid-crystalline molecule consisting of a rigid rod-shaped core with flexible side-chains. Bottom: Chemical structure of 4-cyano-4′-pentylbiphenyl (5CB), one of the best-known representatives of this class of liquid crystals. C) Mesomorphism in thermotropic calamitics and discotics. Calamitic LCs preferably self-assemble in layers, while discotics stack into columnar structures. With increasing temperature, the molecular order decreases until all long-range order is lost in the isotropic melt.

A further distinction is made between thermotropic and lyotropic liquid crystals. This terminology defines the conditions under which a mesophase forms. While thermotropic liquid crystals form mesophases within a certain temperature range without the help of any additive, the formation of lyotropic mesophases requires the aid of a solvent either to provide the necessary fluidity and mobility or to form the anisotropic superstructures, for example in soaps. Owing to the amphiphilicity of lyotropic liquid crystals, they are capable of forming phases different from those of thermotropic LCs. In this Review, we focus on various applications of thermotropic systems. The reader is referred to Ref. [10] for

[*] Dr. E.-K. Fleischmann, Prof. Dr. R. Zentel
Institut für organische Chemie
Johannes Gutenberg-Universität Mainz
Duesbergweg 10–14, 55099 Mainz (Germany)
E-mail: zentel@uni-mainz.de
Homepage: http://www.ak-zentel.chemie.uni-mainz.de

details about capabilities and applications of lyotropic liquid crystals.

Concerning thermotropic mesogens, the liquid-crystalline order is lost in the isotropic melt owing to the thermal motion of the molecules. Upon cooling, the mesogens spontaneously self-organize and adopt a long-range orientational order until a well-ordered crystalline phase is formed at lower temperatures. The mesogens may exhibit several LC phases at different temperatures, which are distinguishable by the degree of order of the mesogens (Figure 1C). The nematic phase is the least ordered mesophase and usually found at the highest temperatures. It is marked by a long-range orientational order of the mesogens, meaning that their only alignment is along one common axis. Additional positional order of calamitic mesogens first appears at lower temperatures within layered smectic phases. In this case, the long axis of the mesogens aligns along the layer normal in a smectic A phase, while they are slightly tilted to the layer normal in a smectic C phase. Additional smectic phases with an improved packing within the layers can exist at even lower temperatures. In comparison, discotic mesogens exhibit positional order by stacking into different types of columnar structures (Figure 1C).[11] The degree of orientational order of the mesogens is described by a dimensionless unit vector, termed the director ***n***. It is quantified as order parameter S [Equation (1)].

$$S = \left\langle \frac{3\cos^2\theta - 1}{2} \right\rangle \quad (1)$$

The parameter S is obtained by averaging the angle θ between the molecular symmetry axis of the mesogens (long axis for calamitic mesogens, short axis for discotics) and the local director over all molecules in a small but macroscopic volume. For an isotropic liquid, the random distribution of angles θ yields an order parameter of $S = 0$. On the other hand, $S = 1$ for a perfectly aligned crystalline state. Typical values from 0.3 to 0.8 are found for calamitic nematic and smectic phases.[12]

The possibility for a smooth transition between a crystalline and an isotropic phase in a stepwise fashion[1,3,13] establishes liquid crystals for a variety of applications that require well-ordered packing over large distances. That is because the director can be aligned macroscopically in the mobile, but less-ordered high-temperature phase (for example nematic) and the local order can be added during slow cooling to more highly ordered (low-temperature) phases. Sharp grain boundaries, which are often found in polycrystalline samples, are not present in a liquid-crystalline phase owing to the ability of the director to continuously change its orientation within the sample. Bending the director of a liquid-crystalline phase requires only little energy and defects are more easily tolerated. Thus, liquid-crystalline phases allow many packing motives that would not be compatible with a regular crystalline lattice.[14,15] In combination with the π-conjugated core of the mesogens, this recommends liquid crystals as active materials for the design of organic semiconducting devices (see Section 2.2).

Owing to the cooperative behavior of the mesogens (parallel orientation of their long axis), liquid-crystalline phases are very sensitive to external fields.[16] They interact as a collective and the effect of switching the director in an applied electric field is many orders of magnitude larger compared to an isotropic liquid, where only the dipole moments of individual molecules interact with the electric field (Kerr effect). In combination with their optical properties (birefringence), liquid crystals can be used to switch the transmittance of polarized light (see Chapters 2 and 6 in particular in Ref. [3]). This effect is exploited for the fabrication of electro-optic displays and forms an integral part in today's display technology.[17]

Compared to crystalline materials, liquid crystals are not only more tolerant towards structural defects but can also host other non-mesogenic units. This allows the synthesis of liquid-crystalline polymers (LCP) and elastomers (LCE), which combine shape-anisotropic mesogens with flexible isotropic polymer chains. In combination with the entropy elasticity of an elastomer network, this gives rise to a stimuli-responsive behavior in slightly cross-linked LCE networks (see Section 3).

2. Liquid-Crystalline Packing and Charge Transport

2.1. Semiconductivity in Liquid Crystals

In general, electronic devices, such as solar cells (photovoltaics), light-emitting diodes (LEDs), and field-effect transistors (FETs) rely on the transport of electrical charges between two electrodes. Inorganic semiconductors, such as crystalline silicon with rather high charge carrier mobility μ, are thus widely used as the charge carrier component. The

Rudolf Zentel is currently Professor at the Institute of Organic Chemistry in Mainz with focus on polymer chemistry and materials science. Since 2006 he is the German speaker of the International Research Training Group "Self-Organized Materials for Optoelectronics", Mainz–Seoul (GRK 1404). His research interests include self-organizing systems (LC-phases or colloids) and the interaction of matter with light.

Eva-Kristina Fleischmann studied chemistry at the Johannes Gutenberg-Universität Mainz and spent an exchange semester at the Technische Universiteit Eindhoven in the group of Prof. Broer. Under the supervision of Prof. Zentel, she recently finished her Ph.D. thesis, which focuses on the microfluidic fabrication of microactuators from liquid-crystalline elastomers.

processing of crystalline silicon is however expensive, and it is difficult to prepare flexible electronic components from the hard material. "Softer" semiconductive organic materials are attractive for the production of flexible and cheaper devices, as they are soluble in organic solvents and can easily be deposited on a substrate. Unfortunately the charge carrier mobility of crystalline inorganic material like silicon cannot be matched by organic semiconductors, where the charges are localized in molecular orbitals of the individual molecules.[18–22]

When discussing charge carrier mobility in organic materials, it is essential to recognize that it is not an intrinsic property of organic molecules. It is a material property and requires hopping of charges between the molecules. For this a sufficient interaction of different π–electron systems (π–π stacking) at the local scale is necessary to allow charge transport between neighboring molecules. With typical stacking distances of several Angstroms, this intermolecular hopping process of charges occurs many times before reaching the opposing electrodes, which have a distance of 100 nm (minimum) to several μm. While closely packed crystalline samples facilitate local charge hopping between organic molecules, grain boundaries in polycrystalline samples strongly affect the charge carrier mobility on a macroscopic scale (Figure 2). In contrast, amorphous films from organic

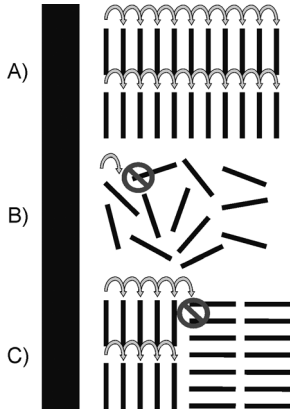

Figure 2. Charge transport in different orientations. A) crystalline: good charge transport, B) amorphous: no charge transport, C) polycrystalline: grain boundaries pin the charges on larger length scales.

materials ($\mu = 10^{-5}$–$10^{-4}\,cm^2\,V^{-1}\,s^{-1}$) suffer from poor local order and weak π-orbital overlap between molecules. Therefore, ideally a monodomain of a properly packed organic material is needed to achieve (relatively) high charge carrier mobilities.

The charge carrier mobility can be measured with two different methods, each possessing a different sensitivity to local and long-range transport processes. Pulsed radiolysis microwave conductivity (PR-TRMC) monitors hopping between a few molecules at a local level[23] and does not discern between the sign of the charge carrier (electron or hole). The macroscopic charge transport is easily overestimated, as this method is insensitive to grain boundaries. Values measured by the time-of-flight (TOF) method on the other hand strongly depend on the occurrence of defects. Furthermore, the type of charge carriers is indicated.[18,24] The first method gives information useful for synthetic chemists interested in an ideal transfer between single molecules, but a comparison between values gained from these two different methods should be avoided.

Liquid-crystalline ordering (Figure 3) offers the possibility to easily orient organic semiconducting molecules[25] and to prepare monodomain samples.[1,3] LC phases possess a higher degree of order than the isotropic melt (amorphous order). It is however lower compared to the perfectly regular and most dense crystal. Thus π-conjugated molecules with liquid-crystalline phases are attractive to improve the charge carrier mobility. In this context discotics were investigated most thoroughly.

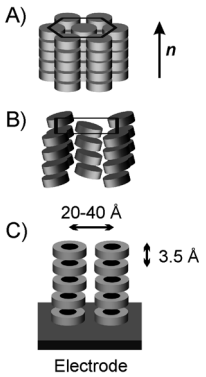

Figure 3. A) Hexagonal assembly of discotic columns (Col_h). B) Columnar rectangular mesophases (Col_r). C) Charge transport in columnar stacked discotics. The aromatic cores (black) form conductive 1D channels, while the surrounding alkyl-chains (gray) act as an insulating layer around the cores.

Discotic phases from large conjugated molecules seem capable of improving the charge carrier mobility. Van der Waals interactions between the aromatic cores and the shape anisotropy of the molecules[26,27] promote the stacking of the mesogens in columnar assemblies. With an average distance of 3.5 Å between the mesogens, the molecular ordering facilitates the interaction of π-orbitals. The charge transport between the mesogens can occur by a repeated hopping process of electrons.[18–21] The charge (electron or hole) then migrates along the long axis of the discotic columns.[28] While any defects or grain boundaries inside a crystalline lattice lower the charge carrier mobility, these are less likely to appear in a liquid-crystalline semiconductor. Instead, the director can bend smoothly over the sample and local defects can be overcome by a self-healing procedure.[29] Thus, the pinning of charge carriers at grain boundaries is much less problematic in organic semiconducting materials with liquid-crystalline order than in polycrystalline samples. In a hexagonal assembly of columns formed by discotic molecules (Col_h), the disk-like molecules are capable of compensating defects by rotating around their short axes and sliding between neighboring columns. This comes at the cost of a decreased overlap of π orbitals, which reduces the charge carrier mobility. In so-called rectangular Col_r phases where the mesogens possess a higher degree of order,[30] the π–π interactions in the discotic columns are considerably stronger

(Figure 3B). Here the mesogens have a fixed position on top of each other. However, the lack of mobility makes them more prone to defects. Their higher density and viscosity also makes them more difficult to handle in a casting process. To counterbalance these features, the orientation step can be done in the less-viscous nematic discotic phase at higher temperatures. A more ordered mesophase necessary for good semiconductivity can then simply be achieved by lowering the temperature of the device.

Flexible aliphatic chains provide the mobility necessary for the discotic phase, but they act at the same time as insulating layer around the stacked columns of aromatic cores, considerably hampering any charge transport between molecules in neighboring columns and promoting an anisotropic electric conductivity.[31] The distance between neighboring columns ranges between 20–40 Å (Figure 3C). The formation of a columnar assembly can thus be seen as a nanosegregation between the conjugated cores and flexible insulating side-chains.[26] As the charge has to move over macroscopic distances (> 100 nm), which is well above the length of an individual undisturbed column, the side-chains become important for macroscopic charge transport as determined by time of flight (TOF) measurements. An increasing length of the side-chains reduces both the packing order among the discotic cores (for example by a transition from a rectangular to a less-ordered hexagonal columnar mesophase) and charge hopping between the columns at the same time.[32] This enhances the lifetime of the charge carriers owing to suppressed recombination[33] but it also strongly reduces charge transport in one dimension (DLCs; molecular wires). This readily illustrates the key problem of DLCs: any discontinuity in a column disrupts the charge motion. Therefore one has to carefully choose from a variety of discotics for use as semiconductors, as the combination of aromatic core, anchoring side-chains, and LC ordering determines the electronic properties of the discotics.[34]

There have been several seminal reviews on the molecular engineering of discotic liquid crystals and their structure–property relationship.[25,30,35,36] Figure 4 illustrates some exemplary aromatic cores, which form the basis for the design of DLCs. The aromatic cores, often with three-, four-, or sixfold rotational symmetry, range from "simple" triazine to more complex structures like phthalocyanine (Pc). The most common procedure for attaching the alkyl side-chains (generally six or more) are nucleophilic or electrophilic substitution reactions at the aromatic core, with the linking groups often being esters, ethers, amides, or alkynes. As a detailed listing of all accomplishments in tailoring discotic LCs is beyond the scope of this review, we will restrict ourselves to a concise summary of state of the art applications of DLCs in electronic devices.

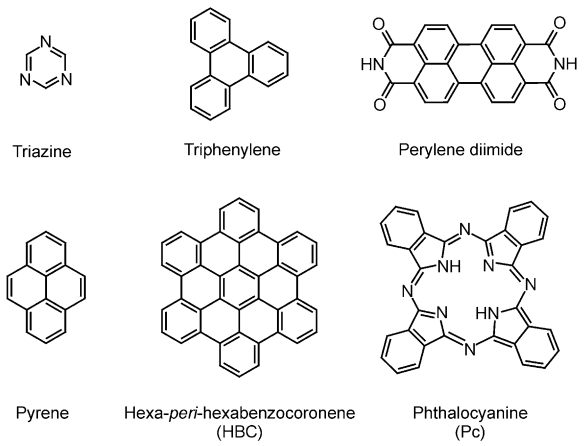

Figure 4. Selection of aromatic cores as rigid moieties in discotic liquid crystals.

2.2. LCs as the Active Component in Opto-electronic Devices

It has roughly been 15 years since the first electronic devices containing discotic liquid crystals were presented. Potential applications range from photovoltaic cells and light emitting diodes to field effect transistors,[37] and the following is a short summary of the results gained to date. Photovoltaic cells and field effect transistors require high charge carrier mobilities for operation, and discotics in particular have been investigated for this purpose. OLED devices on the other hand do not need high charge carrier mobility for operation and can also be made from amorphous semiconducting LC polymers with low charge carrier mobilities.

2.2.1 Organic Light-Emitting Diodes (OLEDs)

The working principle of an organic light-emitting diode (OLED) is light generation by electrical excitation. Electron and hole are injected into the LUMO of the acceptor and HOMO of the donor, respectively, and transported by an applied electric field. Attracted by Coulomb forces, electron and hole combine to form an exciton, which produces luminescence upon relaxation. In a multilayer device, the electron and hole transporting layers are sandwiched between a metal cathode and a transparent indium tin oxide (ITO) anode. In between these layers is the emitter material, the energy levels of which are matched to trap electrons and holes. Similarly to photovoltaic cells, the discotics must adopt a face-on alignment for the best possible charge transport between the electrodes.

Only a handful of discotic systems have been reported for the preparation of OLEDs.[38] Most of the work has been carried out with nematic semiconducting polymers such as certain polyphenylenvinylidene derivatives (PPVs), which form nematic phases owing to their rod-like polymer structure.[39] These systems are known to produce polarized emission parallel to the conjugated polymer chain if the liquid-crystalline phase is macroscopically oriented. This is especially attractive considering that liquid crystal displays (LCDs) nowadays often work with an LED backlight and require polarized light for their operation.

2.2.2 Photovoltaic Cells (PVCs)

Owing to the high charge carrier mobility of inorganic crystalline semiconductors, the photovoltaic effect, that is, the dissociation of an exciton after photon absorption and the

subsequent charge collection of electron and hole at the electrode, is much more pronounced than in organic materials. In the latter, electron and hole are stronger bound to each other because of the lower dielectric constant of the material and the lower charge carrier mobility keeps them close together for a longer time; both effects favor a recombination. Compared to crystalline photovoltaic materials, however, solution-processable organic materials enable the production of thin and flexible solar cells, often in a more cost-effective manner.

An efficient separation of charges and transport to the corresponding electrode requires materials with high charge carrier mobility. Thus liquid-crystalline materials and especially discotics become interesting. Charge separation can be enhanced by blending electron- and hole-transporting materials in a bulk heterojunction (Figure 5). After absorption of photons at the interface of the two materials, the blend ratio must be optimized for a sufficient charge percolation. Bottlenecks and cul-de-sacs in the conducting pathways to the electrodes increase the risk of charge-trapping and recombination of electrons and holes in the active material.[40,41]

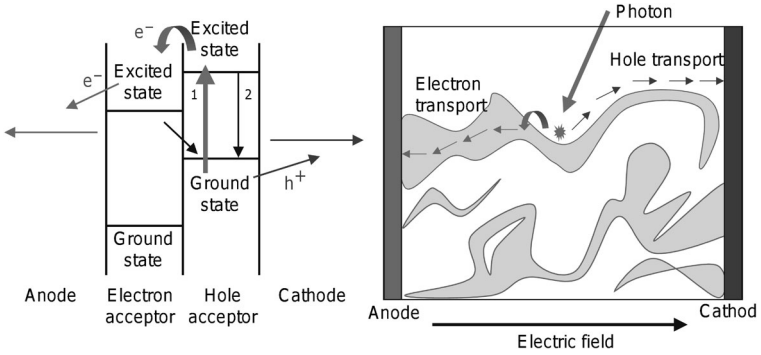

Figure 5. Inner working of an organic photovoltaic cell. Left: After photoexcitation, an efficient charge separation of electron and hole occurs if the changes in energy of ground state and first excited state have the same sign. Right: After photoexcitation at the interface of the two materials, each material must provide a continuous path for the transport of separated charges to the electrodes. Reprinted from Ref. [40] with permission of AAAS.

In 2001, Müllen and co-workers presented the first photovoltaic cell made from a blend of the discotic liquid crystal hexabenzocoronene HBC-PhC_{12} and a perylene dye by a simple solution-processing technique.[42] Exploiting the self-organization of the two components, they formed vertically micro-segregated π-systems with a high interfacial area between the two components. Near 490 nm, the external quantum efficiencies (EQE) were more than 34%, which is a remarkable value for an organic photovoltaic cell.[42,43] An interpenetrating network between hole-accepting (here HBC-PhC_{12}) and electron-accepting (perylene dye) semiconductors is crucial for the preparation of highly efficient photovoltaic devices.[44] For example, the morphology can be controlled and the photovoltaic response improved by annealing HBC/perylene films while in contact with a flat PDMS (polydimethylsiloxane) stamp. These devices exhibit an external quantum efficiency of 29.5% at 460 nm, which is an increase by a factor of two to compared to as-spun films. This effect is attributed to a low overall surface roughness achieved by the top-surface capping structure of the PDMS stamp, which also increases vertical stratification of the two blended semiconductors in the film.[45] Varying the length of the side-chains also influences the resulting morphology, ranging from a layered structure for short side-chains to an increasingly disordered structure with longer side-chains.[46] A photovoltaic cell made by vacuum deposition of a perylene layer on top of a discotic triphenylene ether showed external quantum efficiencies of only 3%. The relatively low EQE is attributed to a non-columnar assembly of the discotic triphenylene ether and the small internal interphase owing to lack of a bulk heterojunction.[47] Further studies of the structure-performance relationship showed that the insulating character of longer substituents reduces the efficiency of electron–hole separation, while short side-chains increase the crystallinity and the performance of the photovoltaic device.[48,49] The performance is additionally enhanced when the columns stack perpendicular to the surface in a so-called face-on or homeotropic alignment.[49] The combination of alignment of the discotics and morphology of acceptor and donor plays a crucial part in the preparation of the photovoltaic cells. Recently the successful preparation of columnar donor and acceptor discotics in a homeotropic alignment in a bilayer-geometry was reported.[50] The organic heterojunction made of two oriented columnar discotics was accessible by judiciously designing the LCs with specific properties. However, no active PVC device was made from this proof-of-principle heterojunction.

Roughly 10 years after the first discotic based PVC was presented, the full capability of this class of materials has not yet been fully exploited. The results so far demonstrate their inherent potential and encourage further research, whether it concerns the relationship between chemical structure and electronic properties, their capability as electron acceptors and donors, or the fabrication processes for building the photovoltaic cells.[51]

2.2.3 *Organic Field-Effect Transistors (OFETs)*

A transistor device consists of a semiconductor and three terminals, which are called source, gate, and drain. Depending on the type of semiconductor used in FETs, either electrons or holes are conducted between source and drain. This drain-to-source current flow is controlled by an applied voltage between source and drain terminal and allows transistors to amplify and switch electronic signals. The applied gate voltage modulates the channel conductivity by either increasing or decreasing the channel size. Columnar DLCs acting as anisotropic charge carriers along the channel can be used as long as they stack parallel to the surface in a planar or edge-on alignment.

This uniaxial alignment of the discotics HBC-PhC_{12} and HBC-$C_{8,2}$ was achieved by *meso*-epitaxial solution growth on oriented PTFE layers. The supramolecularly ordered columnar stacks showed field-effect mobilities of up to

$10^{-3}\,cm^2V^{-1}s^{-1}$ and high on–off ratios of more than 10^4.[52] Highly ordered thin layers of HBC-C_{12} were obtained by employing a zone-casting process (Figure 6B). The corresponding OFETs demonstrated charge carrier mobilities an order of magnitude larger than previously reported for

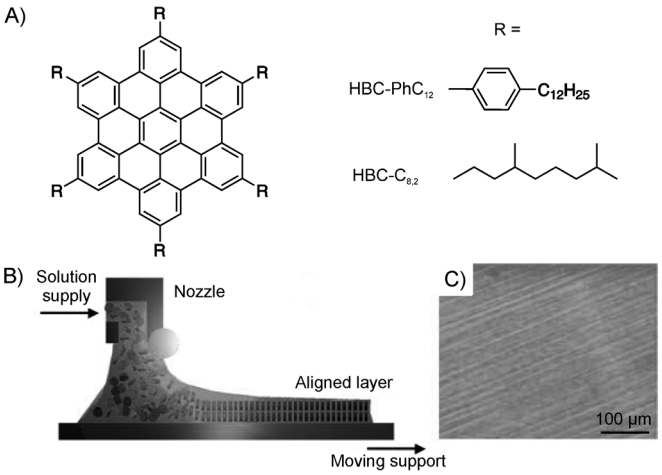

Figure 6. A) Chemical structure of the two HBC derivatives HBC-PhC_{12} and HBC-$C_{8,2}$. B) Zone-casting technique. A solution is spread onto a moving substrate through a nozzle. C) Optical micrograph of zone-casted HBC-C_{12} on a silicon substrate (reflection mode). Reprinted with permission from Ref. [53].

comparable hexabenzocoronene systems.[53,54] Fluorenyl containing hexa-*peri*-hexabenzocoronene (FHBC) derivatives demonstrate improved solubility and are easily spin-cast on OFET devices with a field-effect mobility of up to $2.8\times10^{-3}\,cm^2V^{-1}s^{-1}$.[55] The high number of aromatic cores allows the alignment of the HBC-derivatives with a magnetic field. Such oriented films exhibit field-effect mobilities 10 times larger than FET devices from isotropically aligned films.[56] Spin-coated tetraoctyl-substituted vanadyl phthalocyanine forms highly ordered thin films with edge-on alignment after thermal annealing at 120 °C and exhibits a field-effect mobility of $0.017\,cm^2V^{-1}s^{-1}$.[57] Nanosized FETs can be obtained by integrating single-walled carbon nanotubes (SWNTs) as point electrodes.[58]

An interesting example of how the morphology influences the electronic properties of the semiconductor is given by the discotic dye quaterrylene tetracarboxdiimide. In solution-processed FET devices, where the dye arranges in randomly oriented columns, an ambipolar behavior is observed, that is, electron and hole conductivity with charge carrier mobilities of $1.5\times10^{-3}\,cm^2V^{-1}s^{-1}$ and $1\times10^{-3}\,cm^2V^{-1}s^{-1}$, respectively. Thermal annealing transforms the device into a unipolar electron transporting transistor by increasing the order of the columnar assembly and suppressing hole transport.[59]

Compared to well-established inorganic semiconductors, the class of liquid crystals as semiconductors has been developed quite recently. This is reflected in the charge carrier mobilities, which are two orders of magnitude lower than for the inorganic counterparts. However, charge carrier mobilities as high as $10\,cm^2V^{-1}s^{-1}$ are predicted for defect-free liquid-crystalline assemblies.[60] A better understanding of the structure-property relationship of the liquid crystals can further improve their electronic properties, as demonstrated by an OFET device made of solution-processable ovalene diimide derivatives. Electron mobilities of $1.0\,cm^2V^{-1}s^{-1}$ in nitrogen atmosphere and $0.51\,cm^2V^{-1}s^{-1}$ under oxygen are reported.[61] The ability to tailor components with specific properties and to easily process them in solution makes them a promising alternative to classic inorganic semiconductor materials.

2.3. Alternative Systems for Two- or Three-Dimensional Charge Transport

Discotic phases from large conjugated molecules improve the charge carrier mobility owing to the good overlap of the π-orbitals of the aromatic cores, and high local charge carrier mobilities can be achieved as determined by PR-TRMC (up to $1\times10^{-1}\,cm^2V^{-1}s^{-1}$). The macroscopic charge carrier mobility (accessible by TOF measurements, usually $1\times10^{-3}\,cm^2V^{-1}s^{-1}$) is, however, considerably lower as a result of the sensitivity of the 1D columns to defects.[36,62] In theory, this deficiency can be overcome by 2D smectic layers of calamitic liquid crystals, resulting in an improvement of the charge carrier ability. However it is unlikely that the molecular interactions between the discotics can be matched in a common smectic A or C alignment formed by the small rod-like mesogens, which possess a much smaller conjugated π-system and thus a poorer π–π overlap.[63] Nevertheless, rather high charge carrier mobilities (1×10^{-2} up to $1\times10^{-1}\,cm^2V^{-1}s^{-1}$) over macroscopic distances (TOF measurements) have been reported for smectic terthiophene-based (TTP) molecules, which form smectic E or F phases with three-dimensional order.[64] Given the small conjugated cores of these mesogens, this observation demonstrates the significance of 2- and 3-dimensional charge transport to circumvent naturally occurring defects. The complex nanophase separated columnar structures reported for polyphilic mesogens may lead to a breakthrough.[15,65] To date the research in this field is rather limited, and low-molecular-weight (LMW) calamitics could not yet be established as common semiconductors.

As an alternative to increase the dimensionality of charge transport, polymers with an extended conjugated backbone should be mentioned. With their board-like shape, these rigid polymers pack in a sandic-like fashion, and charge carrier mobilities between 1×10^{-1} and $1\,cm^2V^{-1}s^{-1}$ have been reported.[66] For a detailed discussion of these systems, see Ref. [36]. Another alternative is presented by the recent development in the field of graphene chemistry.[67] Graphene oxides (GO), 2D colloidal systems, are ionically stabilized thin sheets with diameters of several micrometers, while the thickness measures only several nanometers. Their shape resembles that of discotic mesogens, and for aqueous dispersions of single-layered graphene oxide, nematic and lamellar phases were reported,[68] a behavior also known from lamellar clay platelets.[69] This allows their processing from solution to give macroscopic assemblies with long-range order. Subsequent reduction of GO at higher temperatures

gives graphene, which yields high charge carrier mobilities within the sheets.[70] Aggregation and loss of the LC phase of reduced GO can be prevented by the addition of surfactants.[71] These emergent results give a good example of the possibilities, when combining the concept of liquid crystal ordering with systems, which do not contain liquid-crystalline mesogens in the classical sense, whether it be graphene oxide or inorganic nanoparticles, as described in the following chapter.

2.4. Liquid-Crystalline Behavior in Anisotropic Inorganic Nanoparticles

Generally speaking, shape-anisotropic nanoparticles can be seen as oversized mesogens. Densely packed and with enough mobility to reorient, they can form liquid-crystalline phases.[8,9,72] A key process step is to disperse a large enough concentration of these particles in a suitable solvent, despite the need of the particles to minimize their large surface-area to volume ratio by agglomeration. This can be carried out by ionic or steric stabilization methods known from colloid science. In fact, LC phases from ionically stabilized inorganic nanorods have been known since the 1920s.[73] Liquid-crystalline phases from anisotropic nanoparticles allow the combination of the high conductivity of inorganic rod-like semiconductors (for example TiO_2, ZnO) and the orientability of liquid crystals. From the viewpoint of opto-electronics and charge migration (see Section 2.1), the large nanoparticles 1) allow the charge to travel a long way within the nanoparticle at high speed; 2) minimize the hopping steps necessary for macroscopic charge migration due to their large size; and 3) maximize the inter-particle interaction necessary for an optimal hopping process. For photovoltaic applications, blends from donor and acceptor materials are needed. Liquid-crystalline donor–acceptor structures can be obtained by coating the anisotropic inorganic nanoparticle (the acceptor material) with organic polymer chains (the donor material).[74] Furthermore, these sterically stabilized nanoparticles can be processed in solution. In analogy to classical liquid-crystalline mesogens, which are only several magnitudes bigger in size, the anisotropic inorganic core induces the overall orientation, while the flexible polymer chains prevent aggregation and promote the solubility.[75–77]

Blends of nanoparticles and conductive polymers (no chemical linkage, no LC order) have been used in hybrid photovoltaic cells, where the inorganic particles consist of CdSe,[78] TiO_2,[79] and CdTe[80] amongst other materials. Aligning the nanoparticles along a common direction in a polymer matrix to form a heterojunction improves the power conversion compared to bilayer structured solar cells. This effect is due to a larger donor–acceptor interface and minimized charge carrier pathways. The orientation of the nanoparticles could for example be achieved by growth of nanorods directly on the ITO anode by an anodized aluminum oxide (AAO) template[81] or by an electrodeposition process.[80] Exploiting the self-assembly properties of a liquid-crystalline phase offers another pathway for generating aligned semiconducting nanoparticles in a donor matrix. The synthetic route to these hybrid systems is presented in Figure 7.

Controlled radical polymerization allows the design of block copolymers comprised of a short chelating anchor block (for example with catechol groups) and a block providing solubility in different solvents. These block copolymers can be blended with the nanoparticles in a grafting-to fashion.[82] If

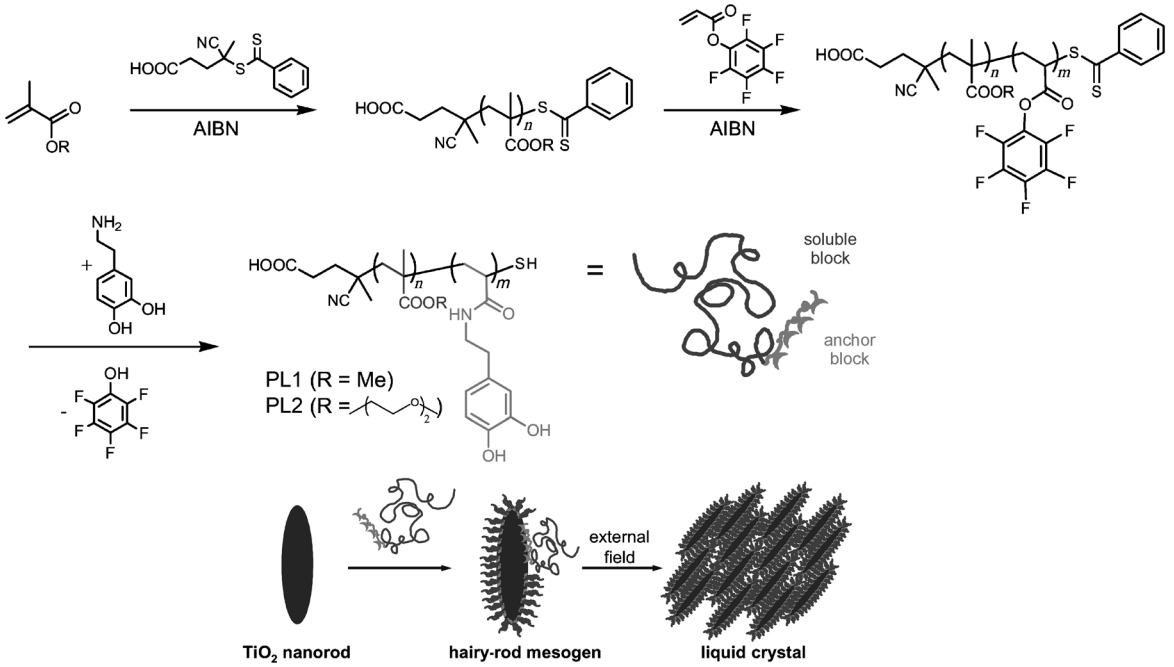

Figure 7. The synthesis of a block copolymer suitable for coating an inorganic nanorod and subsequent LC self-organization of these nanorods owing to their intrinsic anisotropy and polymer chain-mediated mobility. Reprinted with permission from Ref. [75].

the shape anisotropy of the inorganic core is sufficient, liquid-crystalline phases are obtained.[1,3,72] With controlled radical-addition–fragmentation chain-transfer (RAFT) polymerization, a variety of monomers can either be used directly or be introduced into the polymer by a subsequent reaction, which allows direct control over the polymer block length.[75] This approach is applicable to several semiconducting nanoparticles (TiO_2, CdTe, ZnO, SnO_2), and the length and type of polymer block units influences the observed LC behavior of the polymer/nanoparticle hybrids.[77] As previously discussed, a uniform orientation of the nanoparticles is necessary in an active electronic device. This can be achieved by applying methods well known for low-molecular-weight liquid crystals, for example switching between planar and homeotropic alignment with an electric field.[83] Further convective forces in the meniscus on a structured substrate induced an orientation (order parameter $S = 0.7$) in thin films of polymer functionalized TiO_2 and ZnO nanorods during evaporation of the solvent.[84] Recently, electron-conducting nanorods could be coated with a hole conducting component by introducing triarylamine as soluble block into the polymer corona. The obtained hybrid material exhibited LC phases at elevated temperatures, which allowed the orientation of the nanorods by self-assembly.[85] Investigation of these systems by Kelvin probe force microscopy (KPFM) showed a light-induced charge separation between the inorganic nanorod and its hole-transporting polymeric corona, inducing potential differences of some tens of millivolts.[86] Despite the advantageous combination of the electronic properties of inorganic semiconductors with the self-organization of liquid crystals, inorganic nanorod/organic polymer hybrids have not yet been used as active materials in opto-electronic devices.

3. Liquid-Crystalline Order in Networks: Liquid-Crystalline Elastomers

In 1969, Pierre de Gennes was pondering the question as to which benefit might come from the combination of liquid crystals and polymers, imagining an analogue to glass with enhanced elastic properties.[87] It took a couple of years before he proposed a unique feature of such a material: the use of liquid-crystalline elastomers (LCEs) as artificial muscles.[88] These would create macroscopic motion and force owing to processes on a microscopic scale and surpass the response times of by then known pH-responsive polymer networks, because it does not require the transport of solvent in and out of the actuator.[89]

The underlying principle is that the mesogens act as an anisotropic solvent for the isotropic polymer chains. In an isotropic solvent, an undisturbed polymer chain will adopt a spherical random coil conformation with an angle-independent, that is, isotropic radius of gyration.[90] If the polymer is on the other hand mixed with liquid crystals, they will impose their anisotropy on the polymer chain, forcing it into a conformation in which the radius of gyration changes with respect to the director orientation.[91] This distortion may lead to a prolate or oblate chain conformation (Figure 8A). In a prolate conformation, the long axis of the polymer coil

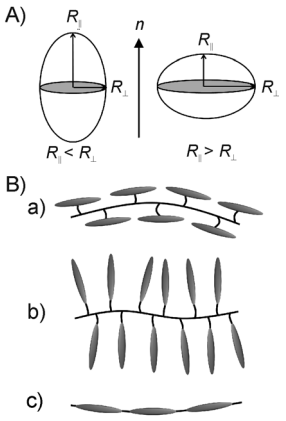

Figure 8. A) Prolate and oblate conformation of the polymer chain due to the liquid crystals acting as anisotropic solvent The radius of gyration *R* changes with respect to the director orientation ***n***. B) Representation of a) side-on, b) end-on side-chain, and c) main-chain polymers.

coincides with the director ($l_\parallel > l_\perp$), while it is perpendicular in an oblate conformation ($l_\parallel < l_\perp$). The mesogens only influence the polymer conformation as long as they are in their liquid-crystalline phase. Upon the phase transition into the isotropic phase, where the order parameter of the mesogens equals zero, the polymer chain is free to revert back to its unperturbed spherical conformation.[92] The reversible phase transition between the mesophase and the isotropic phase of the liquid crystal makes this polymer chain deformation a fully reversible process, which can be exploited for applications such as stimuli-responsive actuators.[93,94] In combination with the elastic reset force of a cross-linked elastomer network, this unique feature can be converted into macroscopic artificial muscles. Several characteristics of an elastomer network have to be considered, namely the type of LC polymers, cross-linking strategies of the LC polymers, sample preparation, and the mode of actuation triggering. This will be discussed in the following sections, chiefly engaging in LC elastomers made from calamitic (rod-like) mesogens.

3.1. Liquid-Crystalline Polymers

As implied above, the influence of the mesogens on the polymer conformation is strongly dependent on the manner of interaction. In fact this effect has only be studied for systems in which mesogens and polymer chains are covalently linked.[95,96] That is because flexible polymers are very poorly soluble in the liquid-crystalline phase of low molar mass liquid crystals. (Low-molar-mass materials might be good solvents in the isotropic phase; the polymer chain precipitates, however, upon cooling into the liquid-crystalline phase.) The length of the spacer dictates the influence of the mesogens on the polymer chain conformation.[97] Longer spacers weaken the coupling between mesogen and polymer, while short spacers increase the shape anisotropy of the polymer chain. Additionally, the position of the spacer with regard to the

mesogens influences the chain anisotropy[98] and consequently the shape-changing properties. Using flexible alkyl chains as spacers, the mesogens can be attached in a side-on or end-on manner to the polymer chain (Figure 8B) and are generally classified as side-chain polymers. Side-on systems promote an orientation of the polymer chain along the director, while two conflicting forces affect the conformation of an end-on polymer. For these comb-like polymers, the anisotropy of the liquid crystal moieties acts along the director field while it simultaneously forces the polymer backbone in a plane perpendicular to it. Thus either prolate or oblate conformations (neutron scattering measurements)[99] have been described for rather similar polymers. As result of this competition, end-on polymers show a weaker chain anisotropy[96] compared to side-on polymers and therefore the corresponding elastomer exhibit weaker contractions upon the isotropic phase transition.[100]

Considering that laterally attached mesogens with short spacers induce a stronger anisotropy of the polymer chain, polymers with mesogens directly integrated into their backbone should show the strongest anisotropy. This has indeed been found for so-called main-chain polymers.[96,101] Main-chain LCEs strongly contract on losing their liquid-crystalline order in the isotropic phase with reported relative length changes of up to 500%.[102]

3.2. Liquid-Crystalline Elastomers

Highly cross-linked networks of LC polymer chains (thermosets) permanently lock-in the liquid-crystalline order of the mesogens. Here the mesogens lack the flexibility to rearrange upon the transition to the disordered isotropic phase and the LC order is preserved up to the decomposition temperature of the network.[103] These dense and highly ordered systems are useless for any actuator application, but exhibit unique optical properties which makes them useful as retarder foils for LC displays, wherein they further improve the color contrast or the viewing angle.[104] For efficient actuation it is essential to increase the flexibility of the mesogens to enable the phase transition with the associated loss of order. This can be achieved in slightly cross-linked LCE samples with elastic moduli of several megapascals (MPa),[105] which is typical for rubbery materials. Thereby, cross-linking can be accomplished in two ways: either by the formation of covalent bonds or by physical cross-linking between the polymer chains.

Supramolecular architectures of LC actuators and sensors can be realized with hydrogen-bonding mesogens.[106] A good example was recently provided by the Ikeda group. A free-standing film of a LC elastomer could be realized by mixing a hydrogen-bond donating LC polymer with a low-molecular weight (LMW) cross-linker, which acts as hydrogen-bond acceptor.[107] Additionally incorporated azobenzenes allowed isothermal switching with UV light. In another example of physical cross-linking, ionic interactions were used to create a weakly cross-linked polymer network by performing an oxidation-reduction reaction on an redox-active LC copolymer.[108]

It is however more common to covalently cross-link the LC polymer chains. A large variety of synthetic methods have been developed over the past 20 years, the main difference being that polymerization and cross-linking are either conducted simultaneously or consecutively.

Simultaneous polymerization and cross-linking allows a conventional bifunctional LMW cross-linker to be used. The cross-linker can either be mesogenic[109] or non-mesogenic,[110,111] as the liquid-crystalline phase is relatively stable towards non-mesogenic impurities. Alternatively, a more stable enantiotropic mesophase can be achieved with a mesogenic cross-linkable polymer, the multi-functionality of which provides for a rapid polymerization and cross-linking.[112] Side-chain elastomers could be realized with polymerizable groups such as acrylates[110] and methacrylates[113] attached to the mesogen. A main-chain elastomer was accomplished by thiol–ene coupling.[114,115]

If cross-linking is carried out in a consecutive step, the polymer precursor is synthesized from mesogenic units and contains either cross-linkable groups or functional groups, which may further react with a cross-linkable LMW component. Polymer precursors with incorporated cross-linkable groups are advantageous for in-bulk preparations of LC elastomers as no additional component is needed for cross-linking. The photoreactive group benzophenone, for example, can already be linked to mesogenic units before polymerization and afterwards cross-link upon irradiation with UV light.[116] Furthermore, cross-linkable groups (such as acrylate, vinyl) can be introduced in a consecutive polymer functionalization and easily be cross-linked in a second step by thermal or photochemical initiation.[117,118] LC polymer chains containing hydroxy groups can be converted with bis(isocyanate)s to yield an elastomer network.[119,120] Elastomers from azide-terminated telechelic side-group LC polymers could be realized by click chemistry, by cross-linking the LC polymer with a LMW triacetylene species.[121]

All of the systems described so far are assembled from classical carbon-based organic molecules, whether in a stepwise fashion or in a one-pot reaction. A different synthetic route is based on polymers with a polysiloxane backbone. An LC polymer is obtained by platinum-catalyzed addition of the vinyl-substituted mesogenic units to the Si–H bond of a siloxane precursor polymer.[122] The ease to choose from a variety of mesogens makes this a modular system, where LC polymers with different compositions and architectures are accessible. Cross-linking can easily be accomplished either during functionalization of the polymer backbone using divinylic cross-linkers[94] or in a consecutive step.[123] It was this method developed and improved by Finkelmann and coworkers, which put actuating LCEs into practice and made it relatively easy to produce macroscopic actuating LCE films.

3.3. Preparation of LCEs and Their Use as Active Devices

While the contraction or expansion of a film is a macroscopic process, it results from the microscopic reorientation of the mesogens and the attached polymer chains. Although liquid crystals self-assemble in the nematic or smectic phase,

the director does not align uniformly throughout the sample. Without an external directing force, polydomains form, with the director being randomly distributed in the elastomer network. When, however, such an external force is applied during cross-linking, the mesogens and thus the polymer chains align along one preferred direction and form a monodomain sample. In the latter case, the loss of orientation in the isotropic phase results in a directed macroscopic shape change of the sample (Figure 9).

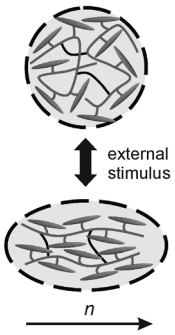

Figure 9. The microscopic loss of order upon the nematic–isotropic phase transition, resulting in a reversible macroscopic shape-change of the slightly cross-linked elastomer.

Fine-tuning the above-described hydrosilylation synthesis, liquid single-crystal elastomers (LSCE), highly ordered LC networks, could be obtained via a two-step cross-linking procedure.[94] Polysiloxane and a judicious mixture of mesogens and cross-linker carrying vinyl as well as methacroyl groups are converted into a weakly cross-linked film. This film is firm enough to be mechanically stretched. This stretching force provides for a uniform orientation of the polymer chains. In a second step, unreacted methacryloyl groups are further converted to yield a fully functional monodomain actuator. A film made with this technique could be incorporated into a microfluidic chip to act as a flow-regulating valve, expanding normal to the director upon the phase transition and thus sealing the microfluidic channel (Figure 10A).[124]

The procedure of mechanical stretching cannot however be adopted to processing reactive LMW mesogens or for the fabrication of micro- and nanoscopic samples. The fabrication of small samples with different geometries is of particular interest for future applications of LCEs as active components in microscopic devices.[125] For LMW mesogens, surface forces are commonly exploited to induce a uniform orientation of the director. The interaction between surface and mesogens may promote a planar (parallel to the surface) or homeotropic (normal to the surface) alignment. A uniform director orientation may simply be induced by microscopic scratches obtained by rubbing of the substrate with cloth. Planar aligned free-standing films could be produced with polyimide-coated substrates.[110,111,126] Surface interactions could also be utilized for the fabrication of nanoactuators made from a main-chain polyester by a mini-emulsion process.[127]

The rigid core of the mesogen, consisting of benzene rings, generate diamagnetism, and can then be aligned with a magnetic field.[118,128] This feature allowed Keller and coworkers to create actuating LCE micropillars by a soft-molding process in a magnetic field (Figure 10B).[115,129]

The director orientation can also be influenced by spatial confinement. Yang et al. used a softlithographic method to prepare a LCE film with a columnar topography. As the diameter of the columns is below the characteristic uniform domain size, the elastomer film adopts a monodomain conformation inside the columns.[130] Similarly, nanoporous anodized aluminum oxide (AAO) templates provide one-dimensional confinement and were used as molds to synthesize wired-shaped nano-LCEs.[131] Such patterned nano- and microstructures created by soft- and photolithography[132] can be used as stimuli-responsive surfaces for micromechanical devices.

The flow field within microfluidic tubing can also induce a preferred orientation in LC droplets. These droplets are prepared at the end of a needle within a T junction and then subjected to shear flow in a thin capillary. The imposed orientation of the mesogens is then permanently fixed by UV-initiated cross-linking. LCE particles with varying shapes are accessible at different flow rates.[133,134] A microfluidic double-emulsion process can be utilized to create core–shell particles, which consist of LCE shells filled with an isotropic liquid core. When the elastomer shell is punctured with a thin capillary, the liquid core is reversibly ejected owing to the deformation of the shell at the phase-transition temperature into the isotropic phase. This process is fully reversible, which allows the core–shell particles to be used as micropumps (Figure 10C).[135]

Along with the sample geometries of films described so far, namely patterned surfaces and particles, it is also possible to create highly ordered LCE fibers (Figure 10D). By simply drawing fibers from a reacting melt of a side-chain polymer and cross-linker with tweezers, the LC polymer spontaneously orients along the fiber axis ($d \approx 300\ \mu m$).[120] The above-mentioned microfluidic procedure is also applicable for the preparation of fibers if the visocity of the solution is high enough to prevent direct decomposition of the liquid jet into droplets. This method could be applied to a cross-linkable main-chain polymer. The fibers created by this wet-spinning process were of a regular thickness between 20–50 μm, depending on the chosen flow rates, and could lift a weight three orders of magnitude higher than their own mass.[136] Even thinner fibers of only several micrometers in diameter are accessible by electrospinning.[137] However, the resulting fleece-like sample, consisting of a chaotic cluster of fibers on top of each other, makes it difficult to extract single fibers for a characterization of their individual properties.

3.4. Stimuli-Responsive LCEs: Not Only Temperature-Dependent

As already explained in the introduction of this Review, the phase transition of thermotropic liquid crystals is triggered by a change in temperature. This most-common actuation was exploited for most of the LCEs presented to date. Admittedly, when integrating LCEs in an active device, it is not advantageous to heat the whole device. Efforts have

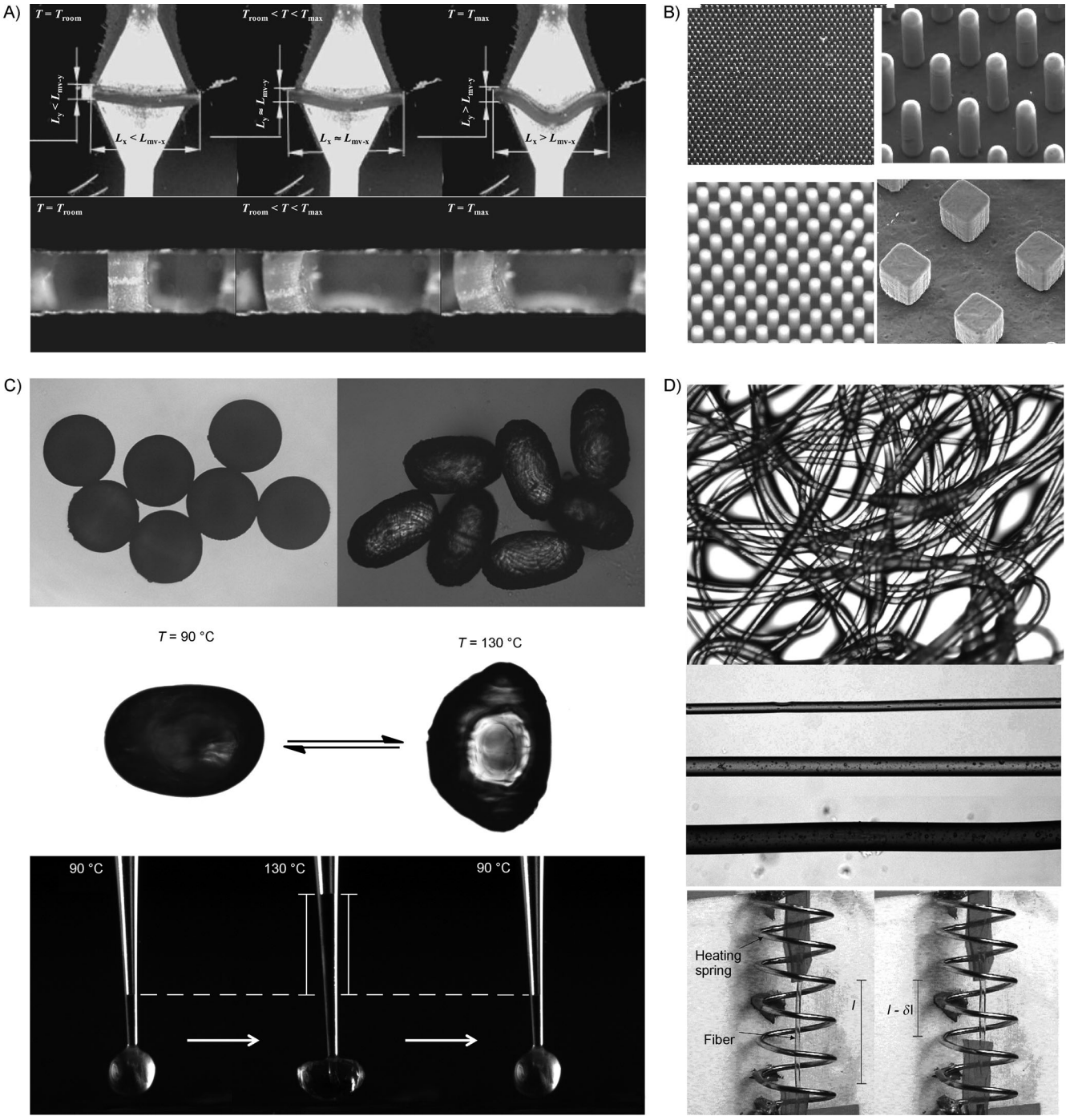

Figure 10. A) An LCE film acts as a flow-regulating valve inside a microfluidic chip. The fluid is allowed to flow while the LCE film is in its glassy nematic state. When heating the LCE film above the nematic–isotropic transition temperature with a copper circuit, the film expands, thus closing the valve and blocking the fluid flow. Reprinted with permission from Ref. [124]. B) The melt of a reactive mesogen is molded inside a PDMS stamp and subsequently polymerized to give LCE micropillars. Reprinted with permission from Ref. [129]. Copyright 2009, American Chemical Society. C) A microfluidic device can be used to prepare bulk and core shell particles, which elongate when heated to the isotropic phase. Punctuated core–shell particles are able to reversibly expel their inner liquid core upon this phase transition and act as a micropump. Reprinted with permission from Ref. [133]. Reprinted with permission from Ref. [135]. Copyright 2012, Nature Publishing Group. D) Top and middle: Continuous fibers produced in a microfluidic device. Reprinted with permission from Ref. [136]. Copyright 2011, Royal Society of Chemistry. Bottom: A fiber drawn from a reactive monomer melt lifts a 200 mg weight. Reprinted with permission from Ref. [120]. Copyright 2003, American Chemical Society.

been made to induce the desired shape change by local heating of the LC-elastomer. Incorporating carbon black allows electrothermal heating of the now conductive LCE with an electric current.[138] Similarly, the introduction of iron oxide particles into the elastomer allows inductive heating with an applied alternating magnetic field.[139] It is also

possible to dope LCEs with carbon nanotubes (CNT). They efficiently absorb visible and infrared light, convert it into local heat, and thus induce the phase transition.[140] The difficulty of producing a stable and homogeneous suspension of CNTs in a liquid-crystalline matrix can be overcome by using a liquid-crystalline polymer surfactant containing pyrene anchoring groups.[141] It could be shown that CNT concentrations below 1% are sufficient for a pronounced actuation of an LCE sample, and that the presence of the dispersed CNT does not significantly affect the LC order or the internal structure of the elastomer.[142] A nematic elastomer in the shape of a cantilever made from such LC-CNT composites exhibited a bending motion on local heating with a laser diode at 660 nm.[143] By creating an elaborate molding process, Camargo and co-workers processed an LCE-CNT film to give a polydomain sample with blister-like monodomain regions (Figure 11). These blister-like shaped monodomain regions contract on irradiation with red light. They could successfully integrate these films into a display, where the localized actuation of the monodomain blisters turns into an active Braille alphabet.[144,145]

Liquid crystals can also be responsive to electric fields if they possess a ferroelectric phase.[146] The electromechanical response is due in this case to the strong macroscopic polarization of the chiral smectic C* phase of the elastomer.[147] For recent summarizations of these ferroelectric liquid-crystalline elastomers (FLCEs), see Refs. [148,149, 150].

Alternatively an isothermal phase transition can be induced by incorporating azo groups into the mesogenic structures, often in the form of azobenzene moieties (Figure 12).[151] The *trans* configuration of the azo group stabilizes the liquid-crystalline alignment of rod-like mesogens. Upon irradiation with UV light at the π–π* absorption band (ca. 360 nm), the photoisomerization from the *trans* to the *cis* configuration of the azobenzene destabilizes the mesophase. The now bent (or kink-like) molecules act as isotropic impurities, which lower the nematic order parameter.[152] This reduces the nematic–isotropic transition temperature to such a degree that an isothermal isotropization becomes possible. A macroscopic shape change of LCEs can be induced at ambient temperatures upon irradiation. The *trans–cis* isomerization can either be reversed by irradiation with visible light (< 470 nm, equivalent to the *n*–π* absorption) or by thermal activation.[153]

A problem of the azo chromophores is their high absorption coefficient. The concentration of azo chromophores (above 5%) necessary to achieve a strong shift of the phase transition temperature entails a high optical density at the surface. Illumination of the sample creates a concentration gradient of the *cis* isomers away from the surface, and this gradient results in a bending motion of the LCE films towards the light source.[111,154] The bending motion creates little stress and cannot be used to lift relatively heavy cargo, but it is very impressive to view. For monodomain samples the bending axis is normal to the director. The Ikeda group could further develop the potential of such films, by making a polydomain LCE film and controlling its bending direction with linear polarized light. Even though the macroscopic orientation of the director was randomly distributed over the whole film, a bending motion parallel to the direction of light polarization was observed.[155]

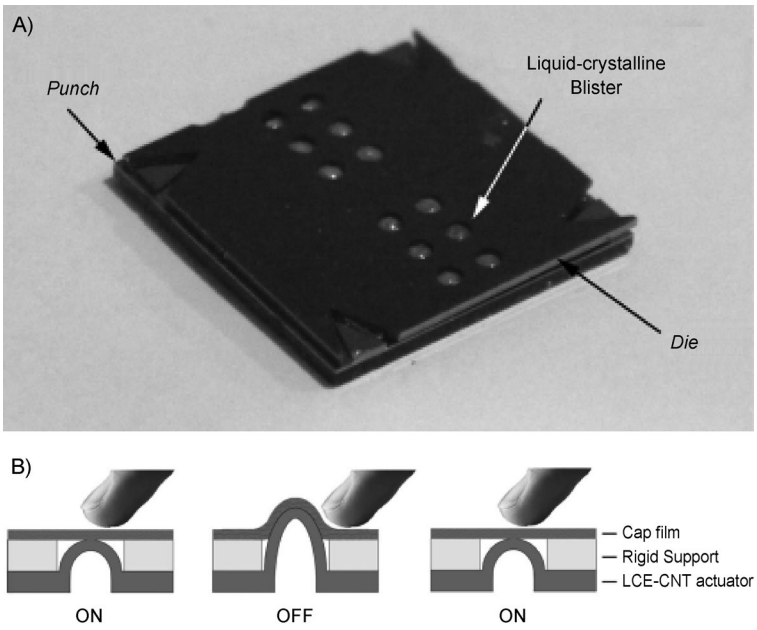

Figure 11. A) A stretched LCE-CNT film is stamped between punch mold and die mold. Also visible are the monodomain blisters. Reprinted with permission from Ref. [145]. Copyright IOP Publishing Ltd. All rights reserved. B) Dynamic Braille dots: The LCE-CNT blister contracts upon irradiation with a light source and becomes unreadable. It recovers its original shape once the light source is turned off. Reprinted with permission from Ref. [145]. Copyright IOP Publishing Ltd. All rights reserved.

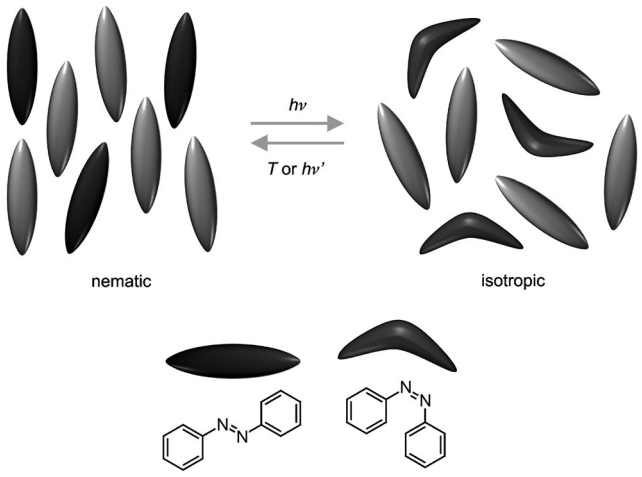

Figure 12. Azobenzene moieties switch from *trans* to the *cis* state upon irradiation with UV light. The kink-like molecules lower the order parameter of the nematic phase, causing an isothermal shift to the isotropic state. The reversibility of this process allows to specifically initiate the shape change of such an LC elastomer by UV irradiation.

Irradiation of a cantilever-shaped sample causes an in-plane bending motion of the cantilever towards the light source, as long as the director is oriented along the long axis of the cantilever. Once the director orientation is rotated with respect to the long axis of the sample, an out-of-plane twisting motion can be observed owing to a shear gradient and contraction along the diagonal of the cantilever.[156] The bending of the photoactive LCEs can further be improved by creating splayed or twisted instead of just planar alignments of the mesogens.[157] The deposition with an ink-jet printer allows different LC materials to be arranged in cantilever-like shape: one sensitive to UV light, the other to visible light. Thus a cilia-like motion can be induced by addressing the different components with their respective wavelength of light (Figure 13 A).[109]

Instead of covalently linking the azo moiety to the elastomer, Palffy-Muhoray and co-workers created LC elastomer network with an azo-dye simply dispersed in it. When floating on water, the material was found to swim into the darker regions, that is, away from the irradiating light source as a result of exchanging momentum between water and the sample upon its bending motion.[158] A light-driven plastic motor was realized by wrapping a photoactive LCE film around two pulleys and illuminating the film with UV light and visible light from two opposing sides. The resulting contraction on one and expansion on the other side results in a rolling motion of the film, which propels the two pulleys (Figure 13 B).[159] The same concept and material could also be used for mimicking the three-dimensional movements of an inchworm walk and a robotic arm motion.[160]

In recent years we could observe significant progress in the fabrication of LCEs, creating elaborate shapes that are capable of performing complex motions. Particularly, the possibility to manufacture micro- and nanosized LCEs allows their integration into lab-on-chip systems. These advances will fuel the transition from fundamental research to competitive commercial applications.

4. Summary and Outlook

We have presented a selection of applications offered by the unique properties of liquid crystals. The combination of order and mobility and the presence of different phases with a different degree of orientation allows the preparation of samples, which combine a long range uniform director orientation with good local packing. This makes liquid-crystalline materials interesting as organic semiconducting materials. Discotic liquid crystals in particular have been investigated in this respect owing to their self-organization

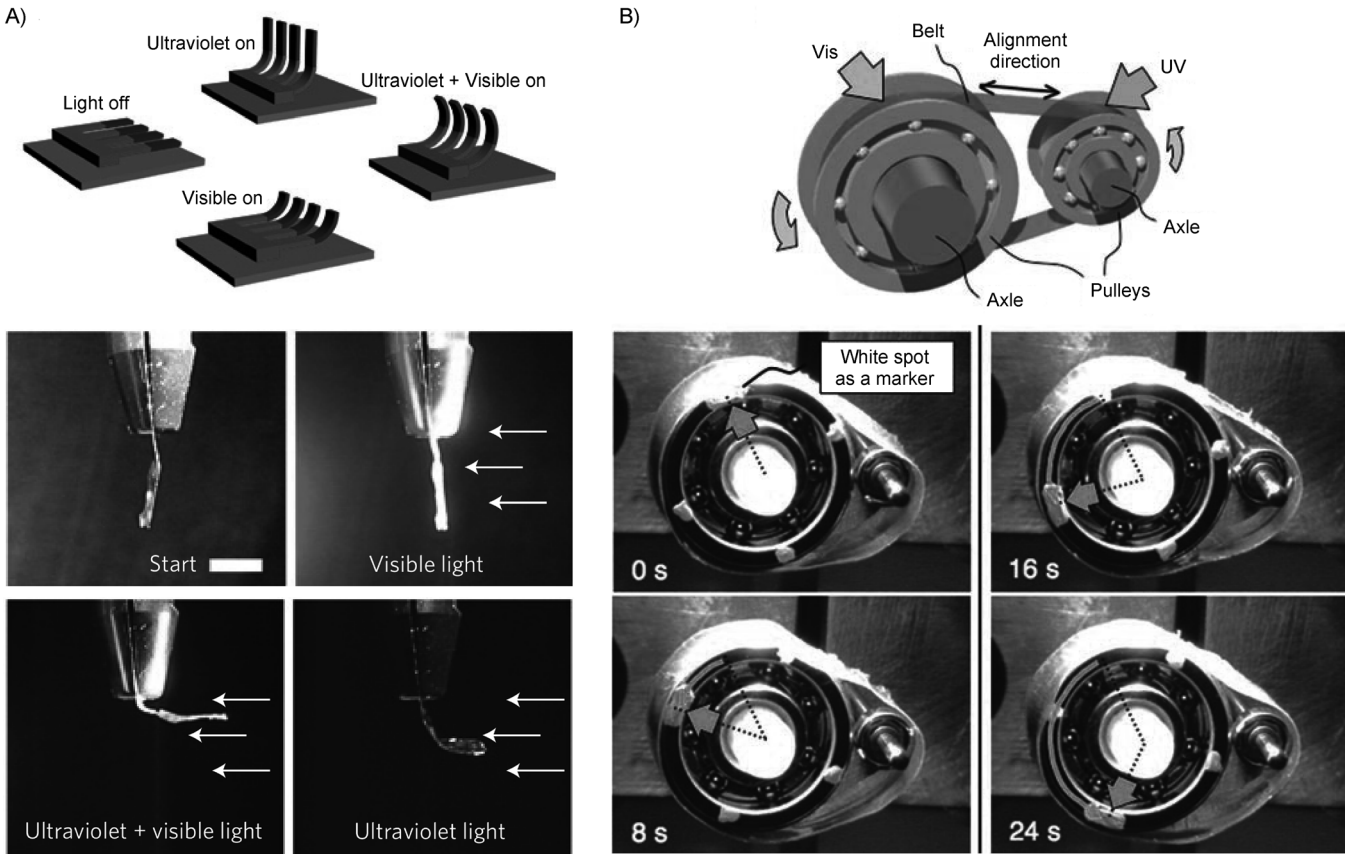

Figure 13. A) Representation and real-life image of a cantilever-like two-component LCE producing asymmetric cilia-like motion depending on the light source. Reprinted with permission from Ref. [109]. Copyright 2009, Nature Publishing Group. B) Top: Representation of a motor laminated with a photoresponsive LCE film. Bottom: By simultaneous irradiation with UV and visible light, the plastic motor is propelled by a bending-unbending movement of the LCE film. Reprinted with permission from Ref. [159].

into semi-crystalline columnar assemblies and the electronic interaction between their aromatic cores. So far, working photovoltaic cells, light-emitting diodes as well as field effect transistors containing DLCs have been accomplished. While several procedures are known to cast uniformly oriented films without defects, it is still a challenge to create multi-layered structures to improve the electron and hole densities and thus the efficiency of the devices. The structural properties of the LCs determine their charge carrier mobility, and much has been achieved in designing discotics with specific electronic properties. A remaining challenge will be to design and synthesize LCs for commercial opto-electronic devices.

Liquid-crystalline elastomers perform a reversible macroscopic shape change upon the microscopic reorientation of mesogens during the nematic–isotropic phase transition. The most common stimulus for triggering this shape change is an increase in temperature. The integration of micro- and even nanosized actuators into elaborate micromechanical devices will however not allow heating of the entire device. For future applications, isothermal stimuli will become more and more important. The integration of photoactive mesogenic units into LCEs has already given rise to remarkable results and is currently judged the most promising candidate for commercial applications.

Along with the broad application of liquid crystals in opto-electronic displays, the concept of liquid-crystalline ordering gives rise to some fundamentally very different technologies. Their use as organic semiconductors and mechanical actuators are only two examples of the scope of liquid-crystalline applications. Furthermore, changes in the director configuration can be exploited for the design of biosensors. Liquid crystals can respond to interaction with for example, protein and lipid domains at LC–aqueous interfaces with changes of the optical and dielectric properties of the LCs, allowing their use for sensor applications.[161] The versatility of liquid crystals in various applications readily illustrates why liquid crystals have remained a research topic with steady interest since their first observation in the 1880s.

The authors like to thank the Deutsche Forschungsgemeinschaft (Ze 230/19) for financial support.

Received: January 15, 2013
Published online: July 23, 2013

[1] D. Demus, J. Goodby, G. W. Gray, H.-W. Spiess, V. Vill, *Handbook of Liquid Crystals Set*, Wiley-VCH, Weinheim, **1998**.
[2] T. J. Sluckin, D. A. Dunmur, H. Stegemeyer, *Crystals that flow, Classic papers from the history of liquid crystals*, Taylor & Francis, London, **2004**.
[3] *Topics in physical chemistry, Vol. 3*, (Ed.: H. Stegemeyer), Steinkopff, Darmstadt, **1994**.
[4] P.-G. de Gennes, *Angew. Chem.* **1992**, *104*, 856; *Angew. Chem. Int. Ed. Engl.* **1992**, *31*, 842.
[5] S. Chandrasekhar, B. K. Sadashiva, K. A. Suresh, *Pramana* **1977**, *9*, 471.
[6] O. Herrmann-Schönherr, J. H. Wendorff, H. Ringsdorf, P. Tschirner, *Makromol. Chem. Rapid Commun.* **1986**, *7*, 791.
[7] T. Niori, T. Sekine, J. Watanabe, T. Furukawa, H. Takezoe, *J. Mater. Chem.* **1996**, *6*, 1231.
[8] J.-C. P. Gabriel, P. Davidson, *Adv. Mater.* **2000**, *12*, 9.
[9] P. Davidson, J.-C. P. Gabriel, *Curr. Opin. Colloid Interface Sci.* **2005**, *9*, 377.
[10] A. G. Petrov, *The lyotropic state of matter*, *Molecular physics and living matter physics*, Gordon & Breach, Amsterdam, **1999**.
[11] C. Destrade, P. Foucher, H. Gasparoux, N. H. Tinh, A. M. Levelut, J. Malthete, *Mol. Cryst. Liq. Cryst.* **1984**, *106*, 121.
[12] J. W. Goodby in *Handbook of Liquid Crystals Set* (Eds.: D. Demus, J. Goodby, G. W. Gray, H.-W. Spiess, V. Vill), Wiley-VCH, Weinheim, **1998**.
[13] G. W. Gray, J. W. G. Goodby, *Smectic liquid crystals*, *Textures and structures*, L. Hill, Glasgow, **1984**.
[14] C. Tschierske, *J. Mater. Chem.* **2001**, *11*, 2647.
[15] C. Tschierske, *Chem. Soc. Rev.* **2007**, *36*, 1930.
[16] G. H. Heilmeier, *Appl. Phys. Lett.* **1968**, *13*, 91.
[17] E. Lueder, *Liquid crystal displays*, *Addressing schemes and electro-optical effects*, Wiley, Chichester, **2010**.
[18] H. Bässler, *Phys. Status Solidi B* **1993**, *175*, 15.
[19] N. Boden, R. Bushby, J. Clements, B. Movaghar, K. Donovan, T. Kreouzis, *Phys. Rev. B* **1995**, *52*, 13274.
[20] H. Cordes, S. Baranovskii, K. Kohary, P. Thomas, S. Yamasaki, F. Hensel, J.-H. Wendorff, *Phys. Rev. B* **2001**, *63*, 094201.
[21] K. Kohary, H. Cordes, S. Baranovskii, P. Thomas, S. Yamasaki, F. Hensel, J.-H. Wendorff, *Phys. Rev. B* **2001**, *63*, 094202.
[22] a) C. D. Dimitrakopoulos, P. R. Malenfant, *Adv. Mater.* **2002**, *14*, 99; b) C. Sheraw, T. Jackson, D. Eaton, J. Anthony, *Adv. Mater.* **2003**, *15*, 2009; c) S. Allard, M. Forster, B. Souharce, H. Thiem, U. Scherf, *Angew. Chem.* **2008**, *120*, 4138; *Angew. Chem. Int. Ed.* **2008**, *47*, 4070.
[23] M. G. Debije, J. Piris, M. P. de Haas, J. M. Warman, Ž. Tomović, C. D. Simpson, M. D. Watson, K. Müllen, *J. Am. Chem. Soc.* **2004**, *126*, 4641.
[24] a) F. Laquai, G. Wegner, H. Bassler, *Philos. Trans. R. Soc. London Ser. A* **2007**, *365*, 1473; b) F. Laquai, G. Wegner, C. Im, H. Bässler, S. Heun, *J. Appl. Phys.* **2006**, *99*, 023712; c) D. Adam, P. Schuhmacher, J. Simmerer, L. Haussling, K. Siemensmeyer, K. H. Etzbachi, H. Ringsdorf, D. Haarer, *Nature* **1994**, *371*, 141.
[25] S. Sergeyev, W. Pisula, Y. H. Geerts, *Chem. Soc. Rev.* **2007**, *36*, 1902.
[26] C. Tschierske, *J. Mater. Chem.* **1998**, *8*, 1485.
[27] J. Barberá, O. A. Rakitin, M. B. Ros, T. Torroba, *Angew. Chem.* **1998**, *110*, 308; *Angew. Chem. Int. Ed.* **1998**, *37*, 296.
[28] a) A. Bayer, S. Zimmermann, J. H. Wendorff, *Mol. Cryst. Liq. Cryst.* **2003**, *396*, 1; b) K. Kohary, H. Cordes, S. D. Baranovskii, P. Thomas, J.-H. Wendorff, *Phys. Status Solidi B* **2004**, *241*, 76.
[29] C. J. Brinker, Y. Lu, A. Sellinger, H. Fan, *Adv. Mater.* **1999**, *11*, 579.
[30] S. Kumar, *Chem. Soc. Rev.* **2006**, *35*, 83.
[31] a) N. Boden, R. J. Bushby, A. N. Cammidge, J. Clements, R. Luo, K. J. Donovan, *Mol. Cryst. Liq. Cryst. Sci. Technol. Sect. A* **1995**, *261*, 251; b) V. S. K. Balagurusamy, S. K. Prasad, S. Chandrasekhar, S. Kumar, M. Manickam, C. V. Yelamaggad, *Pramana J. Phys.* **1999**, *53*, 3.
[32] a) F. Morale, R. W. Date, D. Guillon, D. W. Bruce, R. L. Finn, C. Wilson, A. J. Blake, M. Schröder, B. Donnio, *Chem. Eur. J.* **2003**, *9*, 2484; b) C. K. Lai, C.-H. Tsai, Y.-S. Pang, *J. Mater. Chem.* **1998**, *8*, 1355; c) H. Zheng, C. K. Lai, T. M. Swager, *Chem. Mater.* **1995**, *7*, 2067.
[33] a) J. M. Warman, J. Piris, W. Pisula, M. Kastler, D. Wasserfallen, K. Müllen, *J. Am. Chem. Soc.* **2005**, *127*, 14257; b) P. G. Schouten, J. M. Warman, G. H. Gelinck, M. J. Copyn, *J. Phys. Chem.* **1995**, *99*, 11780.
[34] a) J. M. Warman, M. P. de Haas, G. Dicker, F. C. Grozema, J. Piris, M. G. Debije, *Chem. Mater.* **2004**, *16*, 4600; b) V. Lemaur,

D. A. da Silva Filho, V. Coropceanu, M. Lehmann, Y. Geerts, J. Piris, M. G. Debije, A. M. van de Craats, K. Senthilkumar, L. D. A. Siebbeles, J. M. Warman, J. L. Bredas, J. Cornil, *J. Am. Chem. Soc.* **2004**, *126*, 3271.

[35] a) S. Kumar, *Liq. Cryst.* **2009**, *36*, 607; b) S. Laschat, A. Baro, N. Steinke, F. Giesselmann, C. Haegele, G. Scalia, R. Judele, E. Kapatsina, S. Sauer, A. Schreivogel, M. Tosoni, *Angew. Chem.* **2007**, *119*, 4916; *Angew. Chem. Int. Ed.* **2007**, *46*, 4832; c) B. R. Kaafarani, *Chem. Mater.* **2011**, *23*, 378; d) N. Boden, R. J. Bushby, O. R. Lozman, *Mol. Cryst. Liq. Cryst.* **2003**, *400*, 105; e) S. Chandrasekhar, *Liq. Cryst.* **1993**, *14*, 3; f) S. Bauer, T. Plesnivy, H. Ringsdorf, P. Schuhmacher, *Makromol. Chem. Macromol. Symp.* **1992**, *64*, 19; g) S. Kumar, *Liq. Cryst.* **2004**, *31*, 1037.

[36] W. Pisula, M. Zorn, J. Y. Chang, K. Müllen, R. Zentel, *Macromol. Rapid Commun.* **2009**, *30*, 1179.

[37] a) R. J. Bushby, K. Kawata, *Liq. Cryst.* **2011**, *38*, 1415; b) M. O'Neill, S. M. Kelly, *Adv. Mater.* **2003**, *15*, 1135.

[38] a) I. Seguy, P. Jolinat, P. Destruel, J. Farenc, R. Mamy, H. Bock, J. Ip, T. P. Nguyen, *J. Appl. Phys.* **2001**, *89*, 5442; b) T. Hassheider, S. A. Benning, H.-S. Kitzerow, M.-F. Achard, H. Bock, *Angew. Chem.* **2001**, *113*, 2119; *Angew. Chem. Int. Ed.* **2001**, *40*, 2060; c) M. G. Schwab, T. Qin, W. Pisula, A. Mavrinskiy, X. Feng, M. Baumgarten, H. Kim, F. Laquai, S. Schuh, R. Trattnig, E. J. W. List, K. Muellen, *Chem. Asian J.* **2011**, *6*, 3001; d) I. H. Stapff, V. Stumpflen, J. H. Wendorff, D. B. Spohn, D. Mobius, *Liq. Cryst.* **1997**, *23*, 613; e) G. Lüssem, J. H. Wendorff, *Polym. Adv. Technol.* **1998**, *9*, 443; f) I. Seguy, P. Destruel, H. Bock, *Synth. Met.* **2000**, *111 – 112*, 15.

[39] D. Neher, *Macromol. Rapid Commun.* **2001**, *22*, 1365.

[40] J. Nelson, *Science* **2001**, *293*, 1059.

[41] a) J. Weickert, R. B. Dunbar, H. C. Hesse, W. Wiedemann, L. Schmidt-Mende, *Adv. Mater.* **2011**, *23*, 1810; b) S. Kumar, *Curr. Sci.* **2002**, *82*, 256.

[42] L. Schmidt-Mende, A. Fechtenkötter, K. Müllen, E. Moons, R. H. Friend, J. D. MacKenzie, *Science* **2001**, *293*, 1119.

[43] L. Schmidt-Mende, A. Fechtenkötter, K. Müllen, R. H. Friend, J. D. MacKenzie, *Phys. E* **2002**, *14*, 263.

[44] J. Jung, A. Rybak, A. Slazak, S. Bialecki, P. Miskiewicz, I. Glowacki, J. Ulanski, S. Rosselli, A. Yasuda, G. Nelles, Z. Tomovic, M. D. Watson, K. Mullen, *Synth. Met.* **2005**, *155*, 150.

[45] J. P. Schmidtke, R. H. Friend, M. Kastler, K. Müllen, *J. Chem. Phys.* **2006**, *124*, 174704.

[46] M. Al-Hussein, H. Hesse, J. Weickert, L. Dössel, X. Feng, K. Müllen, L. Schmidt-Mende, *Thin Solid Films* **2011**, *520*, 307.

[47] M. Oukachmih, P. Destruel, I. Seguy, G. Ablart, P. Jolinat, S. Archambeau, M. Mabiala, S. Fouet, H. Bock, *Sol. Energy Mater. Sol. Cells* **2005**, *85*, 535.

[48] J. L. Li, M. Kastler, W. Pisula, J. W. F. Robertson, D. Wasserfallen, A. C. Grimsdale, J. S. Wu, K. Müllen, *Adv. Funct. Mater.* **2007**, *17*, 2528.

[49] H. C. Hesse, J. Weickert, M. Al-Hussein, L. Dössel, X. Feng, K. Müllen, L. Schmidt-Mende, *Sol. Energy Mater. Sol. Cells* **2010**, *94*, 560.

[50] O. Thiebaut, H. Bock, E. Grelet, *J. Am. Chem. Soc.* **2010**, *132*, 6886.

[51] E. Grelet, H. Bock, T. Brunet, J. Kelber, O. Thiebaut, P. Jolinat, S. Mirzaei, P. Destruel, *Mol. Cryst. Liq. Cryst.* **2011**, *542*, 182.

[52] A. van de Craats, N. Stutzmann, O. Bunk, M. Nielsen, M. Watson, K. Müllen, H. Chanzy, H. Sirringhaus, R. Friend, *Adv. Mater.* **2003**, *15*, 495.

[53] W. Pisula, A. Menon, M. Stepputat, I. Lieberwirth, U. Kolb, A. Tracz, H. Sirringhaus, T. Pakula, K. Müllen, *Adv. Mater.* **2005**, *17*, 684.

[54] H. N. Tsao, H. J. Räder, W. Pisula, A. Rouhanipour, K. Müllen, *Phys. Status Solidi A* **2008**, *205*, 421.

[55] W. W. H. Wong, T. B. Singh, D. Vak, W. Pisula, C. Yan, X. Feng, E. L. Williams, K. L. Chan, Q. Mao, D. J. Jones, C. Q. Ma, K. Muellen, P. Baeuerle, A. B. Holmes, *Adv. Funct. Mater.* **2010**, *20*, 927.

[56] I. O. Shklyarevskiy, P. Jonkheijm, N. Stutzmann, D. Wasserberg, H. J. Wondergem, P. C. M. Christianen, A. P. H. J. Schenning, D. M. de Leeuw, Ž. Tomović, J. Wu, K. Mullen, J. C. Maan, *J. Am. Chem. Soc.* **2005**, *127*, 16233.

[57] S. Dong, H. Tian, D. Song, Z. Yang, D. Yan, Y. Geng, F. Wang, *Chem. Commun.* **2009**, 3086.

[58] X. Guo, S. Xiao, M. Myers, Q. Miao, M. L. Steigerwald, C. Nuckolls, *Proc. Natl. Acad. Sci. USA* **2009**, *106*, 691.

[59] H. N. Tsao, W. Pisula, Z. Liu, W. Osikowicz, W. R. Salaneck, K. Müllen, *Adv. Mater.* **2008**, *20*, 2715.

[60] X. Feng, V. Marcon, W. Pisula, M. R. Hansen, J. Kirkpatrick, F. Grozema, D. Andrienko, K. Kremer, K. Müllen, *Nat. Mater.* **2009**, *8*, 421.

[61] J. Li, J.-J. Chang, H. S. Tan, H. Jiang, X. Chen, Z. Chen, J. Zhang, J. Wu, *Chem. Sci.* **2012**, *3*, 846.

[62] A. Tracz, J. K. Jeszka, M. D. Watson, W. Pisula, K. Müllen, T. Pakula, *J. Am. Chem. Soc.* **2003**, *125*, 1682.

[63] X. Crispin, J. Cornil, R. Friedlein, K. K. Okudaira, V. Lemaur, A. Crispin, G. Kestemont, M. Lehmann, M. Fahlman, R. Lazzaroni, Y. Geerts, G. Wendin, N. Ueno, J. L. Bredas, W. R. Salaneck, *J. Am. Chem. Soc.* **2004**, *126*, 11889.

[64] a) H. Iino, J.-I. Hanna, *Mol. Cryst. Liq. Cryst.* **2011**, *542*, 237; b) M. Funahashi, J.-I. Hanna, *Appl. Phys. Lett.* **2000**, *76*, 2574.

[65] a) X. Cheng, X. Dong, G. Wei, M. Prehm, C. Tschierske, *Angew. Chem.* **2009**, *121*, 8158; *Angew. Chem. Int. Ed.* **2009**, *48*, 8014; b) M. Prehm, G. Götz, P. Bäuerle, F. Liu, X. Zeng, G. Ungar, C. Tschierske, *Angew. Chem.* **2007**, *119*, 8002; *Angew. Chem. Int. Ed.* **2007**, *46*, 7856.

[66] M. Ebert, O. Herrmann-Schönherr, J. H. Wendorff, H. Ringsdorf, P. Tschirner, *Liq. Cryst.* **1990**, *7*, 63.

[67] a) C. Cheng, D. Li, *Adv. Mater.* **2013**, *25*, 13; b) J. Kim, L. J. Cote, J. Huang, *Acc. Chem. Res.* **2012**, *45*, 1356; c) J. Wu, W. Pisula, K. Müllen, *Chem. Rev.* **2007**, *107*, 718.

[68] a) B. Senyuk, N. Behabtu, B. G. Pacheco, T. Lee, G. Ceriotti, J. M. Tour, M. Pasquali, I. I. Smalyukh, *ACS Nano* **2012**, *6*, 8060; b) Z. Xu, C. Gao, *ACS Nano* **2011**, *5*, 2908; c) B. Dan, N. Behabtu, A. Martinez, J. S. Evans, D. V. Kosynkin, J. M. Tour, M. Pasquali, I. I. Smalyukh, *Soft Matter* **2011**, *7*, 11154.

[69] D. Kleshchanok, P. Holmqvist, J.-M. Meijer, H. N. W. Lekkerkerker, *J. Am. Chem. Soc.* **2012**, *134*, 5985.

[70] Z. Xu, C. Gao, *Nat. Commun.* **2011**, *2*, 571.

[71] C. Zamora-Ledezma, N. Puech, C. Zakri, E. Grelet, S. E. Moulton, G. G. Wallace, S. Gambhir, C. Blanc, E. Anglaret, P. Poulin, *J. Phys. Chem. Lett.* **2012**, *3*, 2425.

[72] P. J. Flory, *Proc. R. Soc. London Ser. A* **1956**, *234*, 73.

[73] a) L.-S. Li, J. Walda, L. Manna, A. P. Alivisatos, *Nano Lett.* **2002**, *2*, 557; b) H. Zocher, *Z. Anorg. Allg. Chem.* **1925**, *147*, 91.

[74] P. K. Sudeep, T. Emrick, *Polym. Rev.* **2007**, *47*, 155.

[75] S. Meuer, P. Oberle, P. Theato, W. Tremel, R. Zentel, *Adv. Mater.* **2007**, *19*, 2073.

[76] S. Meuer, K. Fischer, I. Mey, A. Janshoff, M. Schmidt, R. Zentel, *Macromolecules* **2008**, *41*, 7946.

[77] M. Zorn, S. Meuer, M. N. Tahir, Y. Khalavka, C. Sönnichsen, W. Tremel, R. Zentel, *J. Mater. Chem.* **2008**, *18*, 3050.

[78] W. U. Huynh, J. J. Dittmer, A. P. Alivisatos, *Science* **2002**, *295*, 2425.

[79] a) K. M. Coakley, M. D. McGehee, *Appl. Phys. Lett.* **2003**, *83*, 3380; b) Q. Qiao, J. T. McLeskey, *Appl. Phys. Lett.* **2005**, *86*, 153501.

[80] Y. Kang, N.-G. Park, D. Kim, *Appl. Phys. Lett.* **2005**, *86*, 113101.

[81] C. Y. Kuo, W. C. Tang, C. Gau, T. F. Guo, D. Z. Jeng, *Appl. Phys. Lett.* **2008**, *93*, 033307.

[82] M. N. Tahir, M. Eberhardt, P. Theato, S. Faiß, A. Janshoff, T. Gorelik, U. Kolb, W. Tremel, *Angew. Chem.* **2006**, *118*, 922; *Angew. Chem. Int. Ed.* **2006**, *45*, 908.
[83] M. Zorn, M. N. Tahir, B. Bergmann, W. Tremel, C. Grigoriadis, G. Floudas, R. Zentel, *Macromol. Rapid Commun.* **2010**, *31*, 1101.
[84] M. Zorn, S. Meuer, M. N. Tahir, W. Tremel, K. Char, R. Zentel, *J. Nanosci. Nanotechnol.* **2010**, *10*, 6845.
[85] M. Zorn, R. Zentel, *Macromol. Rapid Commun.* **2008**, *29*, 922.
[86] a) L. Zur Borg, A. L. Domanski, A. Breivogel, M. Burger, R. Berger, K. Heinze, R. Zentel, *J. Mater. Chem. C* **2013**, *1*, 1223; b) M. Zorn, S. A. L. Weber, M. N. Tahir, W. Tremel, H.-J. Butt, R. Berger, R. Zentel, *Nano Lett.* **2010**, *10*, 2812.
[87] P.-G. de Gennes, *Phys. Lett. A* **1969**, *28*, 725.
[88] a) P.-G. de Gennes, *C. R. Acad. Sci. Ser. IIb* **1997**, *324*, 343; b) P.-G. de Gennes, *C. R. Acad. Sci. Ser. IIb* **1975**, *281*, 101.
[89] A. Katchalsky, *Experientia* **1949**, *5*, 319.
[90] P. Flory, *Statistical mechanics of chain molecules*, Hanser Gardner, Cincinnati, **1989**.
[91] H. Mattoussi, R. Ober, M. Veyssie, H. Finkelmann, *Europhys. Lett.* **1986**, *2*, 233.
[92] a) *Liquid crystallinity in polymers*, *Principles and fundamental properties* (Ed.: A. Ciferri), VCH, New York, **1991**; b) P.-G. de Gennes in *Materials science and technology series* (Eds.: A. Ciferri, W. R. Krigbaum, R. B. Meyer), Academic Press, New York, **1982**.
[93] a) *Advances in polymer science* "*Liquid Crystal Elastomers*: *Materials and Application*" (Eds.: W. H. de Jeu, M. Brehmer), Springer, Berlin, **2012**; b) C. Ohm, M. Brehmer, R. Zentel, *Adv. Mater.* **2010**, *22*, 3366; c) R. Zentel, *Angew. Chem.* **1989**, *101*, 1437; *Angew. Chem. Int. Ed. Engl.* **1989**, *28*, 1407.
[94] J. Küpfer, H. Finkelmann, *Makromol. Chem. Rapid Commun.* **1991**, *12*, 717.
[95] a) H. Finkelmann, *Angew. Chem.* **1987**, *99*, 840; *Angew. Chem. Int. Ed. Engl.* **1987**, *26*, 816; b) C. Boeffel, H. W. Spiess, B. Hisgen, H. Ringsdorf, H. Ohm, R. G. Kirste, *Makromol. Chem. Rapid Commun.* **1986**, *7*, 777; c) A. M. Donald, A. H. Windle, S. Hanna, *Liquid-crystalline polymers*, Cambridge University Press, Cambridge, **2006**.
[96] R. Zentel in *Topics in physical chemistry*, *Vol. 3* (Ed.: H. Stegemeyer), Steinkopff, Darmstadt, **1994**.
[97] a) N. Leroux, P. Keller, M. F. Achard, L. Noirez, F. Hardouin, *J. Phys. II* **1993**, *3*, 1289; b) H. Finkelmann, H. Ringsdorf, J. H. Wendorff, *Makromol. Chem.* **1978**, *179*, 273; c) W. Kaufhold, H. Finkelmann, H. R. Brand, *Makromol. Chem.* **1991**, *192*, 2555.
[98] M. Warner, K. P. Gelling, T. A. Vilgis, *J. Chem. Phys.* **1988**, *88*, 4008.
[99] a) P. Keller, B. Carvalho, J. Cotton, M. Lambert, F. Moussa, G. Pépy, *J. Phys. Lett.* **1985**, *46*, 1065; b) R. G. Kirste, H. G. Ohm, *Makromol. Chem. Rapid Commun.* **1985**, *6*, 179.
[100] F. Moussa, J. Cotton, F. Hardouin, P. Keller, M. Lambert, G. Pépy, M. Mauzac, H. Richard, *J. Phys.* **1987**, *48*, 1079.
[101] F. Hardouin, G. Sigaud, M. F. Achard, A. Brulet, J. P. Cotton, D. Y. Yoon, V. Percec, M. Kawasumi, *Macromolecules* **1995**, *28*, 5427.
[102] S. V. Ahir, A. R. Tajbakhsh, E. M. Terentjev, *Adv. Funct. Mater.* **2006**, *16*, 556.
[103] a) S. N. Bhadani, D. G. Gray, *Mol. Cryst. Liq. Cryst.* **1984**, *102*, 255; b) L. Strzelecki, L. Liebert, *Bull. Soc. Chim.* **1973**, 597.
[104] D. J. Broer, G. P. Crawford, S. Žumer, *Cross-linked liquid-crystalline systems*, *From rigid polymer networks to elastomers*, CRC, Boca Raton, **2011**.
[105] a) R. Zentel, J. Wu, *Makromol. Chem.* **1986**, *187*, 1727; b) T. Pakula, R. Zentel, *Makromol. Chem.* **1991**, *192*, 2401; c) P. Martinoty, P. Stein, H. Finkelmann, H. Pleiner, H. R. Brand, *Eur. Phys. J. E* **2004**, *14*, 311.
[106] D. J. Broer, C. M. W. Bastiaansen, M. G. Debije, A. P. H. J. Schenning, *Angew. Chem. Int. Ed.* **2012**, *51*, 7102.
[107] J.-I. Mamiya, A. Yoshitake, M. Kondo, Y. Yu, T. Ikeda, *J. Mater. Chem.* **2008**, *18*, 63.
[108] A. Wiesemann, R. Zentel, T. Pakula, *Polymer* **1992**, *33*, 5315.
[109] C. L. van Oosten, C. W. M. Bastiaansen, D. J. Broer, *Nat. Mater.* **2009**, *8*, 677.
[110] D. L. Thomsen, P. Keller, J. Naciri, R. Pink, H. Jeon, D. Shenoy, B. R. Ratna, *Macromolecules* **2001**, *34*, 5868.
[111] T. Ikeda, M. Nakano, Y. Yu, O. Tsutsumi, A. Kanazawa, *Adv. Mater.* **2003**, *15*, 201.
[112] E.-K. Fleischmann, C. Ohm, C. Serra, R. Zentel, *Macromol. Chem. Phys.* **2012**, *213*, 1871.
[113] M.-H. Li, P. Auroy, P. Keller, *Liq. Cryst.* **2000**, *27*, 1497.
[114] H. T. A. Wilderbeek, M. G. M. van der Meer, M. A. G. Jansen, L. Nelissen, H. R. Fischer, J. J. G. S. van Es, C. W. M. Bastiaansen, J. Lub, D. J. Broer, *Liq. Cryst.* **2003**, *30*, 93.
[115] A. Buguin, M.-H. Li, P. Silberzan, B. Ladoux, P. Keller, *J. Am. Chem. Soc.* **2006**, *128*, 1088.
[116] a) A. Komp, J. Rühe, H. Finkelmann, *Macromol. Rapid Commun.* **2005**, *26*, 813; b) P. Beyer, E. M. Terentjev, R. Zentel, *Macromol. Rapid Commun.* **2007**, *28*, 1485.
[117] a) M. Brehmer, R. Zentel, *Mol. Cryst. Liq. Crys. A* **1994**, *243*, 353; b) P. Beyer, L. Braun, R. Zentel, *Macromol. Chem. Phys.* **2007**, *208*, 2439.
[118] M.-H. Li, P. Keller, J. Yang, P.-A. Albouy, *Adv. Mater.* **2004**, *16*, 1922.
[119] R. Zentel, M. Benalia, *Makromol. Chem.* **1987**, *188*, 665.
[120] J. Naciri, A. Srinivasan, H. Jeon, N. Nikolov, P. Keller, B. R. Ratna, *Macromolecules* **2003**, *36*, 8499.
[121] Y. Xia, R. Verduzco, R. H. Grubbs, J. A. Kornfield, *J. Am. Chem. Soc.* **2008**, *130*, 1735.
[122] H. Finkelmann, G. Rehage, *Makromol. Chem. Rapid Commun.* **1980**, *1*, 31.
[123] M. Brehmer, R. Zentel, G. Wagenblast, K. Siemensmeyer, *Makromol. Chem.* **1994**, *195*, 1891.
[124] A. Sánchez-Ferrer, T. Fischl, M. Stubenrauch, A. Albrecht, H. Wurmus, M. Hoffmann, H. Finkelmann, *Adv. Mater.* **2011**, *23*, 4526.
[125] H. Yang, G. Ye, X. Wang, P. Keller, *Soft Matter* **2011**, *7*, 815.
[126] K. Urayama, S. Honda, T. Takigawa, *Macromolecules* **2005**, *38*, 3574.
[127] S. Haseloh, C. Ohm, F. Smallwood, R. Zentel, *Macromol. Rapid Commun.* **2011**, *32*, 88.
[128] a) H. Hirschmann, P. M. S. Roberts, F. J. Davis, W. Guo, C. D. Hasson, G. R. Mitchell, *Polymer* **2001**, *42*, 7063; b) M.-H. Li, P. Keller, P.-A. Albouy, *Macromolecules* **2003**, *36*, 2284.
[129] H. Yang, A. Buguin, J.-M. Taulemesse, K. Kaneko, S. Méry, A. Bergeret, P. Keller, *J. Am. Chem. Soc.* **2009**, *131*, 15000.
[130] Z. Yang, G. A. Herd, S. M. Clarke, A. R. Tajbakhsh, E. M. Terentjev, W. T. S. Huck, *J. Am. Chem. Soc.* **2006**, *128*, 1074.
[131] C. Ohm, N. Haberkorn, P. Theato, R. Zentel, *Small* **2011**, *7*, 194.
[132] A. L. Elias, K. D. Harris, C. W. M. Bastiaansen, D. J. Broer, M. J. Brett, *J. Mater. Chem.* **2006**, *16*, 2903.
[133] C. Ohm, C. Serra, R. Zentel, *Adv. Mater.* **2009**, *21*, 4859.
[134] a) C. Ohm, N. Kapernaum, D. Nonnenmacher, F. Giesselmann, C. Serra, R. Zentel, *J. Am. Chem. Soc.* **2011**, *133*, 5305; b) C. Ohm, E.-K. Fleischmann, I. Kraus, C. Serra, R. Zentel, *Adv. Funct. Mater.* **2010**, *20*, 4314.
[135] E.-K. Fleischmann, H.-L. Liang, N. Kapernaum, F. Giesselmann, J. Lagerwall, R. Zentel, *Nat Commun.* **2012**, *3*, 1178.
[136] C. Ohm, M. Morys, F. R. Forst, L. Braun, A. Eremin, C. Serra, R. Stannarius, R. Zentel, *Soft Matter* **2011**, *7*, 3730.
[137] S. Krause, R. Dersch, J. H. Wendorff, H. Finkelmann, *Macromol. Rapid Commun.* **2007**, *28*, 2062.
[138] M. Chambers, H. Finkelmann, M. RemŠkar, A. Sánchez-Ferrer, B. Zalar, S. žumer, *J. Mater. Chem.* **2009**, *19*, 1524.

[139] A. Kaiser, M. Winkler, S. Krause, H. Finkelmann, A. M. Schmidt, *J. Mater. Chem.* **2009**, *19*, 538.
[140] L. Yang, K. Setyowati, A. Li, S. Gong, J. Chen, *Adv. Mater.* **2008**, *20*, 2271.
[141] a) Y. Ji, Y. Y. Huang, E. M. Terentjev, *Langmuir* **2011**, *27*, 13254; b) Y. Ji, Y. Y. Huang, R. Rungsawang, E. M. Terentjev, *Adv. Mater.* **2010**, *22*, 3436.
[142] J. E. Marshall, Y. Ji, N. Torras, K. Zinoviev, E. M. Terentjev, *Soft Matter* **2012**, *8*, 1570.
[143] N. Torras, K. E. Zinoviev, J. E. Marshall, E. M. Terentjev, J. Esteve, *Appl. Phys. Lett.* **2011**, *99*, 254102.
[144] C. J. Camargo, H. Campanella, J. E. Marshall, N. Torras, K. Zinoviev, E. M. Terentjev, J. Esteve, *Macromol. Rapid Commun.* **2011**, *32*, 1953.
[145] C. J. Camargo, H. Campanella, J. E. Marshall, N. Torras, K. Zinoviev, E. M. Terentjev, J. Esteve, *J. Micromech. Microeng.* **2012**, *22*, 075009.
[146] W. Lehmann, H. Skupin, C. Tolksdorf, E. Gebhard, R. Zentel, P. Kruger, M. Losche, F. Kremer, *Nature* **2001**, *410*, 447.
[147] a) E. Gebhard, R. Zentel, *Macromol. Chem. Phys.* **2000**, *201*, 911; b) E. Gebhard, R. Zentel, *Macromol. Chem. Phys.* **2000**, *201*, 902.
[148] S. T. Lagerwall, *Ferroelectric and Antiferroelectric Liquid Crystals*, Wiley-VCH, Weinheim, **1999**.
[149] M. Brehmer, R. Zentel, *Ferroelectric Liquid-crystalline Elastomers*, *Encyclopedia Of Polymer Science and Technology*, Wiley-VCH, Weinheim **2011**.
[150] C. Ohm, M. Brehmer, R. Zentel, *Advances in polymer science* (Ed.: W. H. de Jeu), Springer, Berlin, **2012**.
[151] a) Y. Yu, T. Ikeda, *Angew. Chem.* **2006**, *118*, 5542; *Angew. Chem. Int. Ed.* **2006**, *45*, 5416; b) S. Tazuke, S. Kurihara, T. Ikeda, *Chem. Lett.* **1987**, 911.
[152] T. Ikeda, O. Tsutsumi, *Science* **1995**, *268*, 1873.
[153] a) M. Warner, E. Terentjev, *Macromol. Symp.* **2003**, *200*, 81; b) M.-H. Li, P. Keller, B. Li, X. Wang, M. Brunet, *Adv. Mater.* **2003**, *15*, 569; c) T. Öge, R. Zentel, *Macromol. Chem. Phys.* **1996**, *197*, 1805; d) H. Finkelmann, E. Nishikawa, G. Pereira, M. Warner, *Phys. Rev. Lett.* **2001**, *87*, 015501; e) P. Hogan, A. Tajbakhsh, E. Terentjev, *Phys. Rev. E* **2002**, *65*, 041720; f) J. Cviklinski, A. Tajbakhsh, E. Terentjev, *Eur. Phys. J. E* **2002**, *9*, 427.
[154] Y. Yu, M. Nakano, A. Shishido, T. Shiono, T. Ikeda, *Chem. Mater.* **2004**, *16*, 1637.
[155] Y. Yu, M. Nakano, T. Ikeda, *Nature* **2003**, *425*, 145.
[156] K. M. Lee, M. L. Smith, H. Koerner, N. Tabiryan, R. A. Vaia, T. J. Bunning, T. J. White, *Adv. Funct. Mater.* **2011**, *21*, 2913.
[157] C. L. van Oosten, K. D. Harris, C. W. M. Bastiaansen, D. J. Broer, *Eur. Phys. J. E* **2007**, *23*, 329.
[158] M. Camacho-Lopez, H. Finkelmann, P. Palffy-Muhoray, M. Shelley, *Nat. Mater.* **2004**, *3*, 307.
[159] M. Yamada, M. Kondo, J.-I. Mamiya, Y. Yu, M. Kinoshita, C. J. Barrett, T. Ikeda, *Angew. Chem.* **2008**, *120*, 5064; *Angew. Chem. Int. Ed.* **2008**, *47*, 4986.
[160] M. Yamada, M. Kondo, R. Miyasato, Y. Naka, J.-I. Mamiya, M. Kinoshita, A. Shishido, Y. Yu, C. J. Barrett, T. Ikeda, *J. Mater. Chem.* **2009**, *19*, 60.
[161] a) Y. Bai, N. L. Abbott, *Langmuir* **2011**, *27*, 5719; b) J. M. Brake, *Science* **2003**, *302*, 2094.